

## Intracontinental Quaternary Volcanism in the Niksar Pull-Apart Basin, North Anatolian Fault Zone, Turkey

ORHAN TATAR<sup>1</sup>, SEMA YURTMEN<sup>2</sup>, HALUK TEMİZ<sup>1</sup>, HALİL GÜRSOY<sup>1</sup>,  
FİKRET KOÇBULUT<sup>1</sup>, B. LEVENT MESCİ<sup>1</sup> & JEAN CLAUDE GUEZOU<sup>3</sup>

<sup>1</sup> Cumhuriyet University, Department of Geological Engineering, TR–58140 Sivas, Turkey  
(E-mail: orhantatar@cumhuriyet.edu.tr)

<sup>2</sup> Çukurova University, Department of Geological Engineering, TR–01330 Adana, Turkey

<sup>3</sup> Universitat Cergy Pontoise, 95033 Cergy Pontoise-Cedex, France

**Abstract:** The Niksar Basin is sited along the eastern segment of the North Anatolian Fault Zone in Turkey. It is a young sigmoidal pull-apart basin bordered by two non-parallel master faults associated with earthquakes in 1939 and 1942. The fault geometry along the irregular ENE margin of the basin is complex where young Plio–Quaternary volcanic rocks reach the surface along pairs of steep strike-slip faults which cut the basin sediments. The volcanic rocks around the Niksar Basin have been dated by high precision K-Ar dating and the ages range between  $542 \pm 9$  ka and  $567 \pm 9$  ka. The lavas are mainly alkaline (sodium dominated) in nature and include basaltic trachandesite (mugearite) and trachyandesite (benmoreite) with minor sub-alkaline compositions of dacitic andesite, rhyodacite and rhyolite. Despite the large compositional gap between basaltic and felsic lavas, major and trace element distributions indicate that both the basaltic and felsic lavas are cogenetic. Abundances of major oxides and trace elements vary systematically through this compositional spectrum. Fractional crystallization of the observed phases accounts for the diversity of intermediate and evolved products. Amphibole fractionation in basalts at depth causes the trend towards silica saturation while alkali feldspar fractionation dominates the final stages of crystallization. Significant crustal contamination has occurred in the evolved magmas but contamination is generally minimal or absent in their basaltic parents.

Alkaline basaltic rocks have OIB (ocean island basalt) like trace element patterns characterized by enrichment in LILE, HFSE, LREE and slight depletion in HREE relative to primitive mantle values. Overall geochemical variations indicate the combined effects of different degrees of partial melting, fractional crystallization and variable degrees of crustal contamination.

**Key Words:** Niksar Basin, North Anatolian Fault Zone, intracontinental volcanism, pull-apart basin, strike-slip deformation

### Kuzey Anadolu Fay Zonu (Türkiye) Boyunca Niksar Çek-Ayr Havzasında Kıta İçi Kuvaterner Yaşlı Volkanizma

**Özet:** Kuzey Anadolu Fay Zonu'nun doğu segmentleri üzerinde yer alan Niksar Havzası 1939 ve 1942 depremleri ile ilişkili birbirine paralel olmayan iki ana fay ile sınırlı, genç sigmoidal bir çek-ayır havzadır. Fay geometrisi havzanın düzensiz DKD kenarında karmaşıktır. Burada genç Pliyo–Kuvaterner yaşlı volkanik kayalar havza sedimanlarını da kesen doğrultu-atımlı fay çiftleri boyunca yüzeye çıkmaktadır. Niksar havzası civarında yüzeyleyen volkanik kayalar yüksek hassasiyetli K-Ar yöntemiyle yaşlandırılmış olup, yaşlar  $542 \pm 9$  ka ve  $567 \pm 9$  ka arasındadır. Lavlar çoğunlukla alkalin (sodyumca zengin) özelliindedir ve bazaltik trakiandezit (Mujearit) and trakiandezit (benmorit) ile az oranda sub-alkalin bileşimli dasit, andezit, riyodasit ve riyolitten oluşmaktadır. Bazaltik ve felsik lavlar arasında büyük bir bileşimsel boşluk olmasına rağmen, ana ve iz element dağılımları hem bazaltik hem de felsik lavların eşkökenli olduğunu gösterir. Ana oksitlerin ile iz elementlerin bolluğu sistematik olarak bu bileşimsel dağılım içinde çeşitlilik sunmaktadır. Gözlenen fazlardaki fraksiyonel kristalleşme orta ve ileri derecede gelişmiş ürünlerdeki farklılığı ifade etmektedir. Derinde bazaltlardaki amfibol fraksiyonelleşmesi silikatca doygun bir yönelime neden olurken, alkali feldispat fraksiyonelleşmesi ise kristalleşmenin son evrelerini işaret etmektedir. Belirgin kabuksal kirlenme gelişmiş magma içerisinde oluşmuştur, fakat kirlenme genellikle bunların bazaltik ürünlerinde çok az yada hiç yoktur.

Alkali bazaltik kayalar OIB (okyanus adası bazaltlar) benzeri, LILE, HFSE, LRE zenginleşmesi ve az miktarda ilksel manto değerlerine nazaran azalma gösteren HREE değerleriyle karakterize edilen iz element dağılımları sunmaktadır. Tüm jeokimyasal dağılımlar farklı derecelerdeki kısmi ergime olayının birleşik etkisini, fraksiyonel kristalleşmeyi ve değişik derecelerde kabuksal kirlenmeyi göstermektedir.

**Anahtar Sözcükler:** Niksar Havzası, Kuzey Anadolu Fay Zonu, kıta içi volkanizma, çek-ayır havzası, doğrultu-atımlı deformasyon

## Introduction

The town of Niksar is located at the western edge of a right-stepping overlap region of the North Anatolian Fault Zone. Dextral motion across the main fault is concentrated mainly within a narrow zone incorporating pull-apart basins, but is also laterally distributed over a wider area via a sequence of NE–SW-trending fault splays branching from the main system (Figure 1). These faults segment the crust into a set of large blocks (ca. 5–10 km across) which are believed to be undergoing rotations to accommodate the dextral motion across the block boundary. The overlap region is ca. 8–13 km long and 12 km across and is cut by prominent NE–SW, NW–SE and E–W faults, all showing dextral displacements. The principal displacement direction of the main fault system here is WNW–ESE (Tatar 1993). The oblique basin margins are very irregular, degraded and low in gradient. The topography of the Quaternary plain is ~1 km lower than the surrounding mountain peaks. The basin fill is characterized by active braid-plain, inactive-braid-plain, marsh and alluvial fan/apron deposits, which are thought to be over 600 m in thickness (Tatar 1993).

The 1942 earthquake ( $M_s = 7.0$ ) fault bounds the northern margin of the Niksar pull-apart basin, while the 1939 earthquake ( $M_s = 7.9$ ) fault bounds the southern margin. The strike-slip fault geometry is very complex at the eastern margin of the basin where the main fault segments appear to consist of secondary Riedel shears (Figure 2). Most workers agree that the NAFZ was initiated sometime between Late Miocene and Early Pliocene (e.g., Seymen 1975; Barka & Gülen 1988; Koçyiğit 1989; Tatar 1993; Bozkurt 2001; Westaway 2003; Şengör *et al.* 2005). Estimates of total displacement on the NAFZ have formerly ranged from 7.5 km to 300 km (e.g., Pavoni 1961; Şaroğlu 1985). However, recent studies have established that the total displacement ranges from 10 to 25 km along different parts of the NAFZ (e.g., Barka & Gülen 1988; Koçyiğit 1989; Tatar 1993; Şengör *et al.* 2005).

In tectonically active regions, magmatic activity, or its absence, can be a potential indicator of the stress configuration in the lithosphere. The locations of the volcanism can frequently be related to major fractures in the lithosphere or to intersections of volcano-tectonic lineaments. However, there seems to be no systematic pattern for the distribution of volcanoes in pull-apart basins: in some cases, volcanoes do not occur within the

basin or are sited directly above a buried pull-apart. For example, Late Pleistocene to Recent rhyolite domes in the Coso Range of California occur both within, and up to 8 km outside of, an inferred pull-apart structure (Weaver & Hill 1979).

The centre of a rhomb graben is the site of greatest extension and subsidence across a pull-apart structure (Crowell 1974) where localized crustal stretching and lithospheric extension produce high heat flow and volcanism. Thermal subsidence of the lithosphere around larger pull-apart basins results in extensive overlying sedimentary basins with characteristics similar to those formed above rifts. The thick sedimentary infill in most pull-apart basins tends to: (1) reduce predicted heat flow values; (2) prevent magmas from reaching the surface; and (3) cause the magnetic anomalies produced at orthogonal short ridge segments to be indistinct.

The composition of volcanic rocks reflects their tectonic environment: alkali basalts and tholeiites are formed along continental strike-slip boundaries, while calc-alkaline magmas are typical of strike-slip zones behind arcs and in areas of continental collision (Wilson 1989). The geochemical character of volcanism in pull-apart settings can range from alkaline to tholeiitic and to more differentiated types, including trachytic rocks. The predominance of mafic volcanic activity in such settings suggests that the magmas rise from mantle sources and pass through the crust rapidly enough to prevent extensive crustal melting (Cas & Wright 1987).

## Tectonic Setting of the Young Volcanic Rocks in the Study Area

Occurrences of alkaline volcanism of Pliocene–Quaternary age along the North Anatolian Fault Zone are known in the Erzincan, Suşehri and Reşadiye regions east of the study area (Tatar 1978; Koçyiğit 1989). In the rhomboidal Erzincan Basin along the North Anatolian Fault Zone about a dozen andesitic volcanic cones and many hot springs occur along the traces of both master faults (Aydın & Nur 1982). This volcanism has been related to the initiation of the fault zone. The locations of the volcanic rocks show different characteristics within each basin. A number of young volcanic cones are observed in the easternmost part of the Niksar Basin along the master faults (Ketin 1969) and range from Late Miocene to Quaternary in age (Seymen 1975). To the

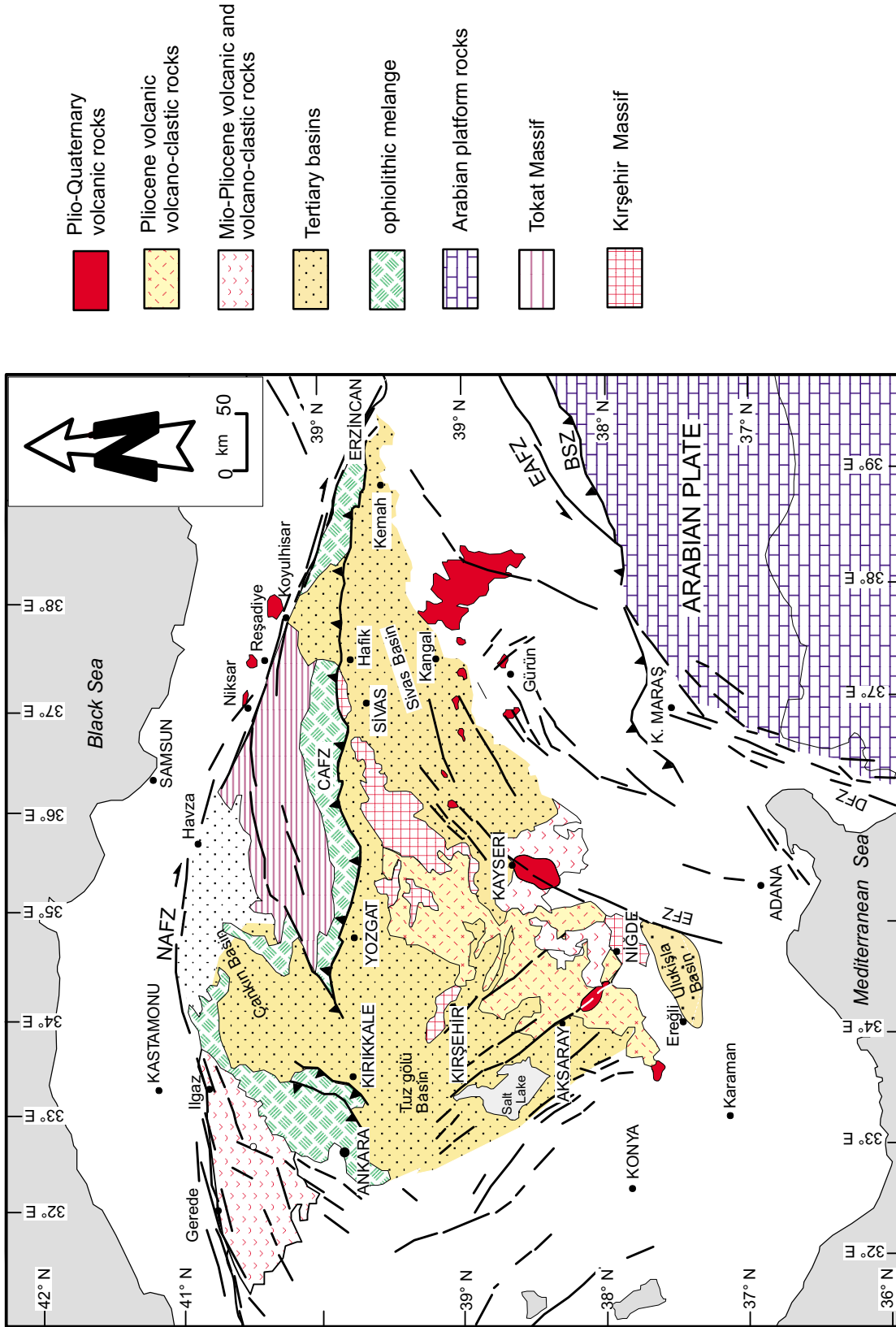


Figure 1. Regional location map illustrating pull-apart basins within the North Anatolian Fault System in central-east Turkey. The splay faults (Bozkurt & Koçyiğit 1996) branch from the main fault zone (simplified from 1:2,000,000 Turkish Geological Map). The insert shows the regional location within the plate framework of Turkey. Abbreviations: BSZ– Bitlis Suture Zone, DFZ– Dead Sea Fault Zone, NAFZ– North Anatolian Fault Zone, EAFZ– East Anatolian Fault Zone, EFZ– Ercemiş Fault Zone, CAFZ– Central Anatolian Fault Zone.

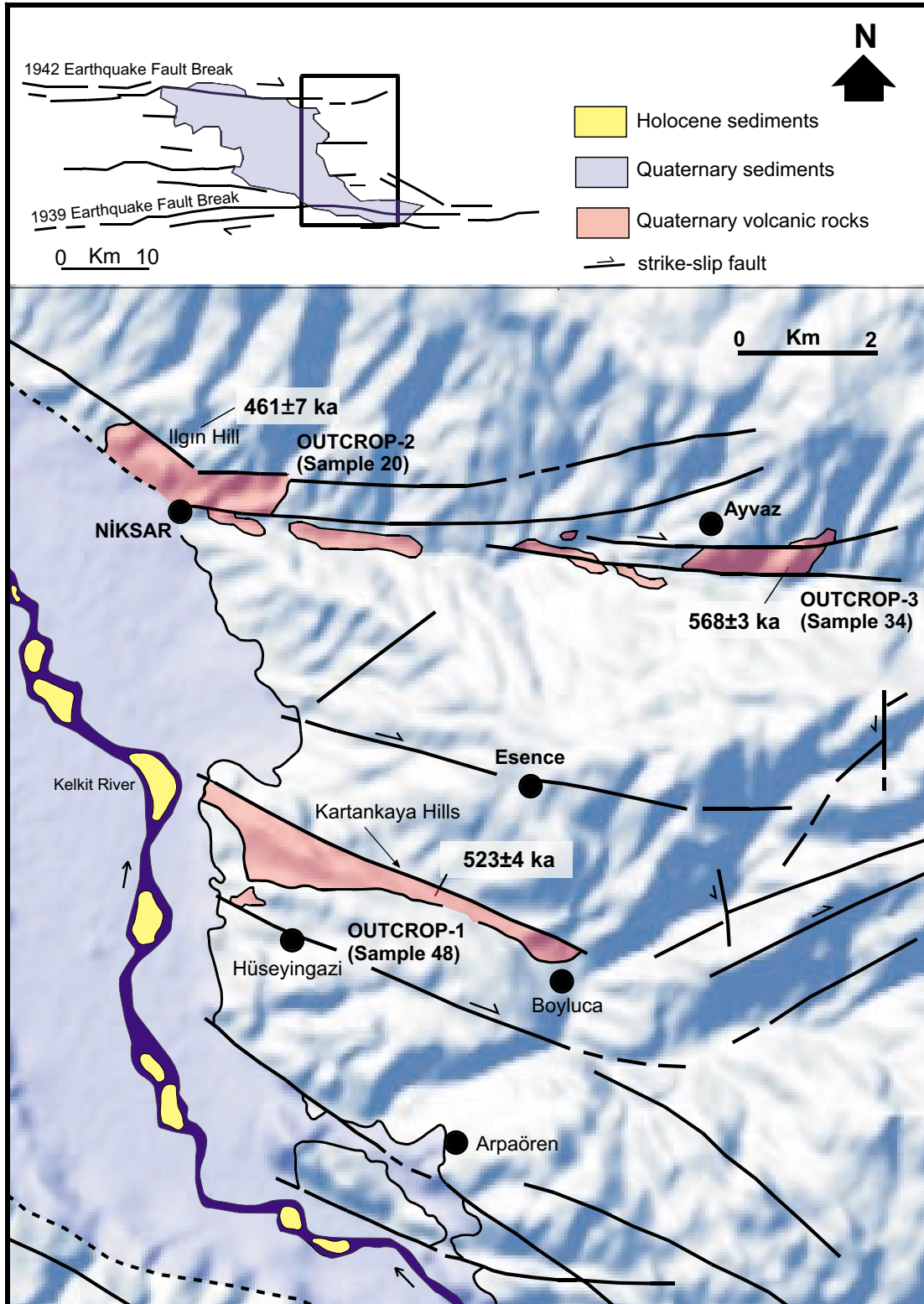


Figure 2. Geological, geographical and age distribution of the young volcanic rocks around the Niksar Basin. Inset map shows the general tectonic setting of the Niksar Basin.

east, the Pliocene sediments in the Suşehri Basin are cut by basaltic to rhyolitic dykes. This study describes the three main outcrops of young volcanic rocks in the Niksar pull-apart basin immediately to the west of Reşadiye and Suşehri basins (Figure 1).

### *Radiometric Dating*

Radiometric dating on these young volcanic rocks has been carried out at the CEA-CNRS Laboratory in Yvette, in France. High precision K-Ar whole rock age determinations from three different lavas range from  $568 \pm 3$  ka to  $461 \pm 7$  ka and define a Middle Pleistocene age. Sample 20 from Niksar quarry is dated at  $461 \pm 7$  ka. Sample 48 from the fault-bounded Kartankaya Hills is dated at  $523 \pm 4$  ka and sample 34 from the eastern part of Niksar town within the Çanakçı valley yielded a determination of  $568 \pm 3$  ka. The locations of the dated units are shown in Figure 2 and volcanic outcrop descriptions are given in the following sections.

*Hüseyingazi-Boyluca.* The volcanic rocks in this area are located southeast of Niksar town near the villages of Hüseyingazi and Boyluca (outcrop 1 in Figure 2). The outcrop is bounded on the north by a  $115^\circ$  N-trending strike-slip fault dipping at  $72^\circ$  N. Flow features indicate southeastward flow onto a young valley floor. At the southern margin of the outcrop, the lavas unconformably overlie the northern flank of a syncline comprising deformed Upper Cretaceous red limestones. At the northern side of the outcrop, Quaternary deposits rest on the fault-bounded young volcanic rocks. The relationship of the volcanic rocks to the fault and to the filling of a young valley floor by younger deposits suggests that volcanic rocks here could be related to initiation of the intracontinental fault zone.

*North of Niksar.* The second outcrop is located to the north of Niksar town (outcrop 2) in a transtensional zone between two strike-slip faults (Figure 2). These faults trend in two different directions, to the north of Niksar, they strike  $125^\circ$  N and, then change eastwards to roughly E–W. The southwestern edge of the outcrop is bordered by the 1942 earthquake fault break which terminates in the western part of Niksar town. Basin-fill deposits rest on the volcanic rocks to the south and east.

However, the volcanic rocks overlie Upper Cretaceous limestones and Eocene volcanic rocks in the north.

Palaeomagnetic studies indicate a clockwise rotation of up to  $20^\circ$  here; this rotation appears to be related to the initiation of the fault zone because regional rotations immediately to the north are anticlockwise (Tatar *et al.* 1995). The extension that caused the magma to reach the surface would then have occurred before rotation (Tatar *et al.* 1992).

*Ayvaz Location.* The third outcrop is the smallest, and located along one of the splay faults near the southern part of Ayvaz village (outcrop 3, 4 in Figure 2); this lies in Çanakçı river valley within a feature interpreted as transtensional (Tatar *et al.* 1990). The northern side of the outcrop is bordered by a  $095^\circ$  N-trending strike-slip fault along which 425 m of displacement has been identified (Tatar 1993).

These volcanic rocks at outcrops level 3 have directions of magnetisation consistently directed  $240$ – $270^\circ$  N. Although magnetic inclinations are not entirely diagnostic of polarity, they are positive and almost certainly normal. They identify rapid clockwise rotation at rates in excess of  $50^\circ/\text{m.y.}$  Recognition of comparable declinations and probable normal polarity at all of the lavas associated with this young pull-apart basin support results of the K-Ar study in showing that igneous activity here has been confined to the Bruhnes chron ( $<0.78$  m.y.); this would also account for the lack of burial (Tatar *et al.* 1995; Piper *et al.* 1996).

### **Petrography and Chemical Characteristics of the Volcanic Rocks**

#### *Analytical Methods*

Whole rock samples were analysed on a fully automated ARL 8420 x-ray fluorescence spectrometer at the School of Earth Science and Geography, Keele University. Major oxide analyses used fused glass beads with a 1:5 mixture of ignited sample and lithium metaborate flux; trace element analyses used pressed powder pellets. Analytical details are given in Floyd & Castillo (1992). The spectrometer, with a rhodium x-ray tube, has been calibrated against ~40 international and internal rock standards of appropriate compositions. Precision has been determined by pooled variance on the results obtained

from replicate analyses on individual samples. The error for major oxides is generally 1.0%–1.5% (except 0.6% for  $\text{SiO}_2$  and total Fe as  $\text{Fe}_2\text{O}_3$ ) and most trace elements to within ~5%. However concentrations of rare earth elements are unreliable if below ~30 ppm.

### Classification of the Volcanic Rocks

The young volcanic rocks in the Niksar pull-apart basin have been classified by using the total alkali versus silica diagram ( $\text{Na}_2\text{O} + \text{K}_2\text{O}$  wt% vs  $\text{SiO}_2$  wt%) of Le Bas *et al.* (1986) (Figure 3). They classify as basaltic trachyandesite (or mugearites), trachyandesite (or benmoreite), andesitic dacite, dacite, rhyodacite and rhyolites. The volcanic rocks have also been plotted on the total alkali vs silica diagram of Irvine & Baragar (1971) to indicate their alkaline and sub-alkaline nature (Figure 4). The most mafic rocks including mugearites and benmoreites are alkaline containing both normative nepheline (up to ~7%) and normative olivine (up to ~11.4%), whereas intermediate to acid rocks including andesitic dacites, dacites, rhyodacites and rhyolites are sub-alkaline.

The samples from Hüseyingazi-Boyluca form a trend with a significant compositional gap in their silica content from mugearite to rhyodacite and rhyolite. The samples from north of Niksar also form an alkaline to sub-alkaline trend from mugearite to benmoreite, dacitic andesites and dacites. The Ayvaz location samples are of restricted composition and classified as mugearite and benmoreite. In general, the Niksar pull-apart basin volcanic rocks show a compositional trend towards silica-oversaturated composition similar to those of the continental sector of the Cameroon line volcanic rocks (Fitton 1987). They also show close similarities to the many Tertiary/Quaternary intraplate magmatism of Central Europe (Wilson & Downes 1991; Wilson *et al.* 1995) and of Turkey (Parlak *et al.* 1997, 1998, 2001; Polat *et al.* 1997; Arger *et al.* 2000; Yurtmen *et al.* 2000).

### Petrography

The sub-alkaline dacites, rhyodacites and rhyolites are typically porphyritic and composed of plagioclase, quartz, alkali feldspar, biotite and hornblende phenocrysts set in

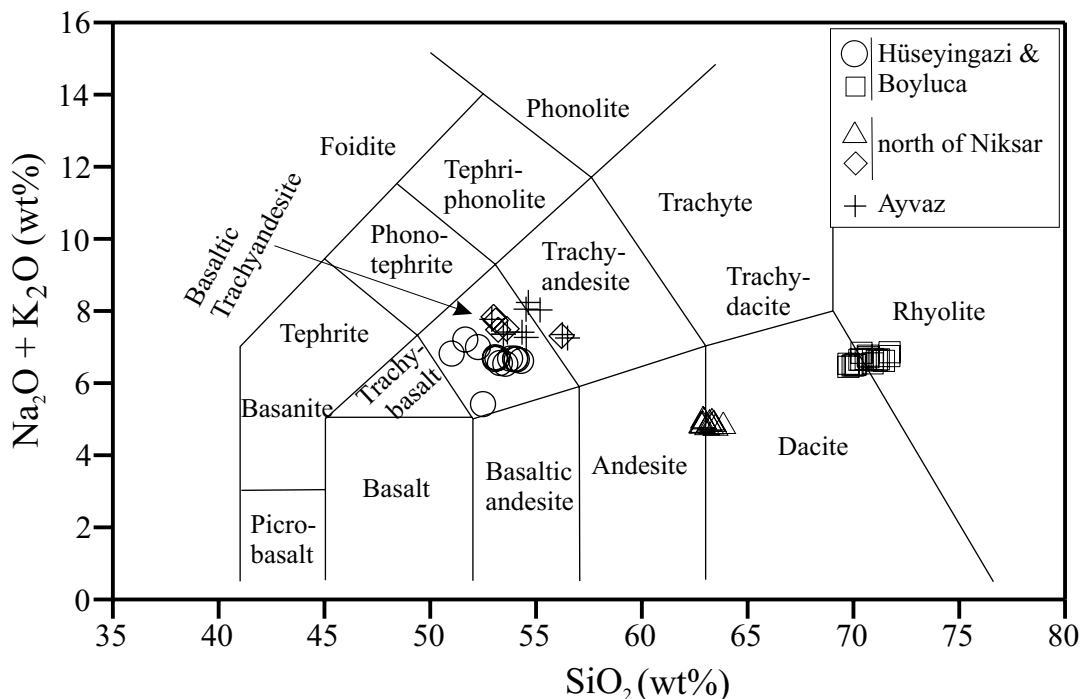


Figure 3. Classification of the Niksar pull-apart basin volcanic rocks in the TAS diagram of Le Bas *et al.* (1986). H– Hüseyingazi (outcrop 1), N– Niksar (outcrop 2), A– Ayvaz (outcrop 3).

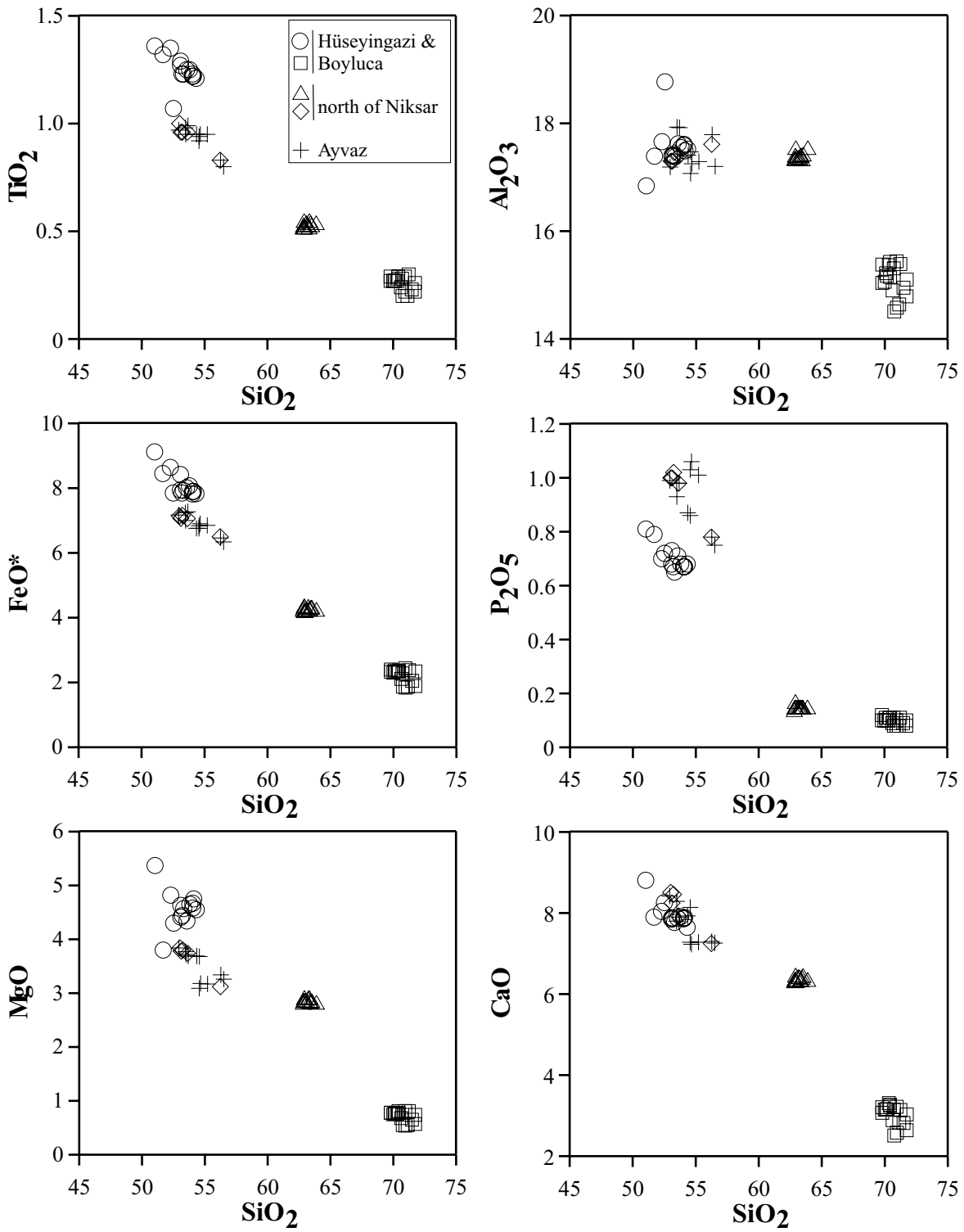


Figure 4. Alkaline and sub-alkaline nature of the Niksar pull-apart basin volcanic rocks in Irvine & Baragar (1971) diagram.

a fine-grained groundmass of plagioclase, quartz, alkali feldspar and glass. Plagioclase phenocrysts are zoned and of albite-oligoclase in composition. Some have resorbed margins sometimes overgrown by small and non-resorbed equilibrium plagioclase. Subhedral and rounded quartz phenocrysts also show resorption textures. Localized flow texture is evident by elongate biotite crystals. Some radial intergrowths of quartz and alkali feldspar arranged around euhedral plagioclase phenocrysts are present.

Porphyritic andesites and dacitic andesites have plagioclase, ortho- and clino-pyroxene phenocrysts. They also contain amphibole phenocrysts which mainly show hybrid breakdown alteration. The amphiboles may be entirely substituted by pyroxene and iron-oxide minerals.

Mugearites and benmoreites are mineralogically similar and mainly consist of euhedral or subhedral and completely altered pyroxene and plagioclase phenocrysts. The groundmass is texturally microporphyritic and/or trachytic and consists of minute elongate plagioclase, small pyroxenes and magnetite. Rare pseudomorphs of amphibole and quartz xenocrysts surrounded by pyroxene granules are also present.

### *Major and Trace Element Chemistry*

Major and trace element compositions of selected representative samples of the Niksar pull-apart basin volcanic rocks are presented in Table 1.

Major element variations were evaluated using  $\text{SiO}_2$  contents of the rocks as a differentiation index (Figure 5). The most striking feature of these diagrams is the three fold grouping of lavas into a mafic mugearite-benmoreite group, an intermediate andesite-andesitic dacite group and a felsic rhyodacite-rhyolite group with each group being separated by a well-defined composition gap (Figure 3). Almost all the alkaline lavas are nepheline normative (0.35–6.98 Ne). Dacites, rhyodacites and rhyolites have high normative quartz (~17–30 Q). Major and trace element variations in  $\text{SiO}_2$  diagrams show well-defined and regular curvilinear trends that generally reflect the phenocryst contents (Figure 5). This can be explained in terms of fractional crystallization. In these diagrams  $\text{FeO}^*$ , MgO, CaO,  $\text{TiO}_2$  and  $\text{P}_2\text{O}_5$  show very good negative correlations and all decrease regularly with differentiation (Figure 5).  $\text{Al}_2\text{O}_3$  displays curvilinear trends and in mugearites and benmoreites increases with

increasing  $\text{SiO}_2$  whilst decreasing in intermediate and felsic lavas with increasing  $\text{SiO}_2$ ; this indicates that the combined effect of clinopyroxene and plagioclase fractionation controls the formation of the mugearites and benmoreites. The dacites and rhyolites are highly evolved and exhibit fractionation effects of Fe-Ti oxides and alkali feldspar. The Niksar pull-apart basin basic lavas have  $\text{Na}_2\text{O}/\text{K}_2\text{O}$  ratios between 1.9 and 3.4. This ratio decreases in more evolved magmas owing to separation of amphibole and plagioclase. The  $\text{Na}_2\text{O}/\text{K}_2\text{O}$  ratio of the rhyolites is between 1.7 and 2.1.

Distributions of selected trace elements relative to  $\text{SiO}_2$  (as a differentiation index) are shown in Figure 6. Sr, Zr, Nb and Y show scattered negative and Rb scattered positive correlations with silica. The transition metals (Cr, Ni, V) show marked continuous depletion with silica throughout the series but continuous positive correlation with MgO. Again high valence cations (Th, Nb, Zr) are correlated with other alteration resistant elements (Sr, Y, La) and scattered but definite positive correlations observed in these diagrams (Figure 7). This indicates that the Niksar pull-apart basin volcanic rocks were enriched by these elements during the partial melting and fractional crystallization.

The Sr content is significantly higher in the mafic lavas than in the felsic lavas. The range of Sr contents of the mugearites and benmoreites is between 803 and 1348 ppm. In dacites it is between 364 and 369 and in the rhyolites between 240 and 289 ppm. Sr shows a consistent decrease with increasing  $\text{SiO}_2$  indicating the dominance of plagioclase fractionation.  $\text{CaO}/\text{Al}_2\text{O}_3$  ratios decrease very regularly with decreasing MgO content (Figure 8) and this can be explained by fractionation of pyroxene and plagioclase. Zr and Nb generally show covariance in basaltic and felsic lavas.

The distinct nature of the low-silica (alkaline) and high-silica (sub-alkaline) group is also evident by certain incompatible trace element ratios such as Ba/Nb, Zr/Nb, Th/Y and Nb/Y (Table 1). The low silica alkaline group is characterized by high Nb/Y (1.41–2.55) and low Ba/Nb (9.28–19.91), Zr/Nb (4.23–5.71), Th/Y (0.12–0.59). In contrast, the high silica subalkaline group is represented by high Th/Y (0.53–1.00), Ba/Nb (28.6–79.63), Zr/Nb (12.00–21.38) and low Nb/Y (0.53–1.00). This indicates that the low silica alkaline rocks show geochemical characteristic features of lavas from mid-plate extensional settings and are similar to those observed in number of

Table 1. Whole-rock major and trace element data for the representative samples from Nixsar pull-apart basin.

Sample	Hüseyingazi and Boyluca																					
	Alkaline								Calc-alkaline													
SiO <sub>2</sub> wt%	51.68	51.03	52.28	53.57	52.51	53.09	54.31	53.08	53.31	53.2	53.8	54.11	54.03	54.04	0.45	95-1	95-2	95-3	95-4	95-6	95-7	95-8
TiO <sub>2</sub>	1.32	1.36	1.35	1.25	1.07	1.29	1.21	1.27	1.23	1.23	1.25	1.22	1.22	1.23	0.29	0.22	0.24	0.2	0.22	0.27	0.27	0.2
Al <sub>2</sub> O <sub>3</sub>	17.39	16.84	17.66	17.62	18.77	17.41	17.52	17.39	17.38	17.41	17.55	17.49	17.61	17.59	15.38	14.58	14.9	14.64	14.79	15.04	15.17	14.51
Fe <sub>2</sub> O <sub>3</sub> <sup>t</sup>	8.45	9.12	8.64	8.01	7.85	8.42	7.83	7.94	7.93	7.85	8.07	7.9	7.89	7.82	2.4	1.84	2.11	1.87	1.89	2.33	2.33	1.87
MnO	0.15	0.16	0.15	0.13	0.14	0.14	0.13	0.13	0.14	0.13	0.14	0.13	0.13	0.13	0.06	0.04	0.05	0.04	0.05	0.04	0.04	0.04
MgO	3.8	5.37	4.82	4.34	4.3	4.41	4.55	4.63	4.57	4.44	4.65	4.75	4.58	4.67	0.78	0.54	0.68	0.55	0.57	0.78	0.76	0.55
CaO	7.9	8.81	8.04	7.87	8.26	7.88	7.65	7.85	7.77	7.87	7.91	7.89	7.87	7.86	3.07	2.58	2.89	2.83	2.64	3.21	3.15	2.51
N <sub>2</sub> O	4.86	4.5	4.73	4.42	4.2	4.59	4.63	4.65	4.51	4.66	4.65	4.66	4.67	4.68	4.34	4.19	4.4	4.3	4.43	4.33	4.4	4.32
K <sub>2</sub> O	2.37	2.34	2.29	2.14	1.24	2.15	2.01	2.04	2.07	2.05	2.05	2.02	2.03	1.99	2.22	2.5	2.29	2.35	2.34	2.14	2.14	2.42
P <sub>2</sub> O <sub>5</sub>	0.79	0.81	0.7	0.71	0.72	0.73	0.68	0.68	0.65	0.67	0.68	0.67	0.67	0.67	0.12	0.08	0.09	0.08	0.08	0.1	0.1	0.08
LOI	0.97	0.03	-0.24	0.3	1.44	-0.01	-0.22	-0.16	0	0.01	-0.09	-0.16	-0.22	-0.2	1.34	1.8	1.91	2.05	1.88	1.66	1.58	2.08
Total	99.68	100.37	100.42	100.37	100.48	100.1	100.3	99.51	99.57	99.53	100.7	100.7	100.5	100.4	99.8	99.34	100.17	100.05	100.62	99.7	100.11	99.33
Rb ppm	43	42	36	40	11	43	38	42	41	40	44	42	42	39	74	77	75	84	79	66	70	80
Sr	945	1097	870	803	1014	879	826	837	798	826	828	820	830	823	279	244	263	252	260	285	284	240
Ba	647	628	529	548	677	599	542	522	552	516	514	514	518	524	589	651	589	637	637	571	603	636
Nb	57	56	57	50	34	56	50	52	51	51	51	49	51	50	9	9	9	8	9	8	8	9
Th	6	3	7	6	3	9	9	10	10	8	10	12	13	10	20	12	14	12	12	12	11	11
Y	26	26	24	23	24	26	24	24	24	24	20	22	22	23	17	14	14	14	13	15	14	14
Ni	31	46	31	41	59	38	39	43	40	43	41	38	40	42	3	2	5	5	2	5	2	1
Cr	20	78	20	32	44	40	37	46	44	41	49	47	39	43	11	16	17	15	15	15	15	16
Pb	8	10	9	6	4	20	16	18	17	19	20	19	18	18	6	23	20	25	18	18	20	20
V	94	132	107	112	58	119	104	116	106	118	114	114	112	107	15	19	29	21	18	30	25	25
Zn	88	89	85	84	86	89	81	84	84	89	88	79	84	84	44	43	45	44	41	43	43	41
Zr	245	237	247	230	194	243	218	231	230	230	229	223	227	225	172	142	154	145	145	167	167	143
La	57	51	42	41	44	57	57	50	57	47	50	47	52	52	25	10	17	23	23	23	17	23
Ce	99	99	98	76	118	92	93	85	87	91	102	91	81	80	33	42	40	28	34	41	29	40
Nd	41	31	33	28	55	30	33	33	43	39	40	33	34	42	16	32	21	16	14	23	19	15
Zr/Nb	4.3	4.23	4.33	4.6	5.71	4.34	4.36	4.44	4.51	4.51	4.49	4.55	4.45	4.5	19.11	15.78	17.11	18.13	16.11	20.88	20.88	15.89
Y/Nb	0.46	0.46	0.42	0.46	0.71	0.46	0.48	0.46	0.47	0.47	0.39	0.45	0.43	0.46	1.89	1.56	1.56	1.75	1.44	1.88	1.75	1.56
Ba/La	11.4	12.3	12.6	13.4	15.4	10.5	9.5	10.4	9.7	11	10.3	10.9	10	10.1	23.6	65.1	34.6	27.7	27.7	24.8	35.5	27.7
Th/Nb	0.1	0.1	0.1	0.1	0.1	0.2	0.2	0.2	0.2	0.2	0.2	0.2	0.3	0.2	2.2	1.3	1.6	1.5	1.3	1.5	1.4	1.2
La/Nb	1	0.9	0.7	0.8	1.3	1	1.1	1	1.1	0.9	1	1	1	1	2.8	1.1	1.9	2.9	2.6	2.9	2.1	2.6
Al <sub>2</sub> O <sub>3</sub> /TiO <sub>2</sub>	13.2	12.4	13.1	14.1	17.5	13.5	14.5	13.7	14.1	14.2	14	14.3	14.4	14.3	53	66.3	62.1	73.2	67.2	55.7	56.2	72.6
N <sub>2</sub> O/K <sub>2</sub> O	2.1	1.9	2.1	2.1	3.4	2.1	2.3	2.3	2.2	2.3	2.3	2.3	2.3	2.4	2	1.7	1.9	1.8	1.9	2	2.1	1.8
CaO/Al <sub>2</sub> O <sub>3</sub>	0.45	0.52	0.46	0.45	0.44	0.45	0.44	0.45	0.45	0.45	0.45	0.45	0.45	0.45	0.2	0.18	0.19	0.19	0.18	0.21	0.21	0.17
CaO/TiO <sub>2</sub>	5.98	6.48	5.96	6.3	7.72	6.11	6.32	6.18	6.32	6.4	6.33	6.47	6.45	6.39	10.59	11.73	12.04	14.15	12	11.89	11.67	12.55

Table 1. Continued.

Sample	Hüseyingazi and Boyluca										North of Nilsar										
	Calc-alkaline										Calc-alkaline										
	95-9	95-10	95-11	95-12	95-13	95-14	95-15	95-16	95-17	0-54	95-18	95-19	95-20	95-21	95-22	95-23	95-24	95-25	95-26	95-27	95-28
SiO <sub>2</sub> wt%	70	70.1	71.24	70.41	70.32	70.72	70.95	71.75	70.42	62.93	62.92	62.98	63.24	63.52	63.44	63.12	63.35	63.89	62.84	62.89	63.32
TiO <sub>2</sub>	0.27	0.27	0.3	0.29	0.27	0.28	0.29	0.26	0.28	0.55	0.52	0.52	0.53	0.53	0.54	0.54	0.55	0.54	0.52	0.53	0.52
Al <sub>2</sub> O <sub>3</sub>	15.06	15.22	15.39	15.43	15.37	15.31	15.44	15.1	15.15	17.55	17.34	17.38	17.36	17.43	17.34	17.37	17.41	17.55	17.35	17.41	17.41
Fe <sub>2</sub> O <sub>3</sub> <sup>t</sup>	2.3	2.37	2.38	2.33	2.34	2.28	2.44	2.34	2.37	4.37	4.22	4.22	4.35	4.33	4.32	4.26	4.26	4.26	4.26	4.32	4.28
MnO	0.04	0.04	0.04	0.03	0.03	0.03	0.03	0.02	0.03	0.07	0.06	0.06	0.06	0.06	0.06	0.06	0.06	0.06	0.06	0.06	0.06
MgO	0.75	0.77	0.81	0.81	0.76	0.74	0.81	0.74	0.78	2.92	2.87	2.86	2.91	2.86	2.84	2.86	2.86	2.83	2.83	2.87	2.92
CaO	3.15	3.16	3.14	3.24	3.31	3.15	3.22	3.03	3.27	6.47	6.35	6.33	6.43	6.46	6.41	6.43	6.35	6.36	6.33	6.38	6.36
Na <sub>2</sub> O	4.4	4.27	4.3	4.39	4.37	4.41	4.27	4.35	4.49	3.82	3.77	3.88	3.8	3.68	3.8	3.74	3.83	3.74	3.77	3.76	3.72
K <sub>2</sub> O	2.11	2.25	2.38	2.28	2.3	2.37	2.3	2.53	2.37	1.26	1.18	1.17	1.19	1.19	1.18	1.15	1.19	1.18	1.17	1.17	1.19
P <sub>2</sub> O <sub>5</sub>	0.1	0.11	0.11	0.11	0.1	0.11	0.1	0.1	0.11	0.17	0.15	0.15	0.15	0.15	0.15	0.15	0.15	0.15	0.14	0.15	0.15
LOI	1.39	1.4	0.43	0.4	0.35	0.4	0.43	0.38	0.38	-0.08	0.03	-0.05	-0.08	-0.06	-0.08	-0.07	0.6	-0.08	0.62	0.63	0.34
Total	99.57	99.96	100.5	99.7	99.51	99.79	100.29	100.6	99.46	100.03	99.42	99.45	99.95	100.1	99.99	99.62	100.6	100.4	99.89	100.17	100.28
Rb ppm	69	67	67	66	66	66	69	74	71	37	37	37	37	37	37	38	37	37	37	37	37
Sr	286	287	281	286	289	280	284	266	282	369	369	369	366	369	367	368	365	368	366	369	364
Ba	582	601	607	608	613	593	601	613	585	291	294	291	279	284	296	290	288	270	286	279	279
Nb	8	8	8	8	8	8	8	9	9	9	9	9	9	9	9	9	9	10	9	10	9
Th	11	12	12	11	11	10	11	11	12	11	6	6	6	6	4	5	3	5	6	3	4
Y	15	13	14	14	14	13	15	15	15	12	10	10	10	11	11	11	11	10	10	10	11
Ni	2	2	4	4	4	4	3	4	3	30	31	31	29	30	29	30	28	30	31	31	30
Cr	15	21	17	16	20	13	14	17	16	31	30	31	33	33	33	32	31	33	31	29	30
Pb	17	18	18	20	17	18	16	22	20	3	17	15	17	17	16	16	15	17	13	15	14
V	27	37	33	34	30	27	35	30	33	83	79	94	83	82	87	87	85	83	80	87	91
Zn	43	42	42	43	41	42	43	43	44	52	53	53	54	53	52	50	52	53	53	54	53
Zr	168	169	171	170	171	166	169	165	174	117	118	118	121	120	119	120	120	120	119	120	120
La	17	17	11	27	17	20	17	23	17	18	8	13	17	20	13	20	17	20	20	17	10
Ce	49	42	27	40	24	45	32	27	39	40	27	21	37	28	40	36	43	31	36	23	43
Nd	20	23	10	12	15	12	16	22	14	18	13	12	23	14	23	13	22	14	17	14	21
Zr/Nb	21	21.13	21.38	21.25	21.38	20.75	21.13	18.33	19.33	13	13.11	13.11	13.44	13.33	13.22	13.33	13.33	12	13.22	12	13.33
Y/Nb	1.88	1.63	1.75	1.75	1.75	1.63	1.88	1.67	1.67	1.33	1.11	1.11	1.11	1.22	1.22	1.22	1.22	1.11	1.11	1	1.22
Ba/La	34.2	35.4	55.2	22.5	36.1	29.7	35.4	26.7	34.4	16.2	36.8	22.4	16.4	14.2	22.8	14.8	17.1	14.4	13.5	16.8	27.9
Th/Nb	1.4	1.5	1.5	1.4	1.4	1.3	1.4	1.2	1.3	1.2	0.7	0.7	0.7	0.7	0.4	0.6	0.3	0.5	0.7	0.3	0.4
La/Nb	2.1	2.1	1.4	3.4	2.1	2.5	2.1	2.6	1.9	2	0.9	1.4	1.9	2.2	1.4	2.2	1.9	2	2.2	1.7	1.1
Al <sub>2</sub> O <sub>3</sub> /TiO <sub>2</sub>	55.8	56.4	51.3	53.2	56.9	54.7	53.2	58.1	54.1	31.9	33.3	33.4	32.8	32.9	32.1	32.2	31.7	32.5	33.4	32.8	33.5
Na <sub>2</sub> O/K <sub>2</sub> O	2.1	1.9	1.8	1.9	1.9	1.9	1.9	1.7	1.9	3	3.2	3.3	3.2	3.1	3.2	3.3	3.2	3.2	3.2	3.2	3.1
CaO/Al <sub>2</sub> O <sub>3</sub>	0.21	0.21	0.2	0.21	0.22	0.21	0.21	0.2	0.22	0.37	0.37	0.36	0.37	0.37	0.37	0.37	0.36	0.36	0.36	0.37	0.37
CaO/TiO <sub>2</sub>	11.67	11.7	10.47	11.17	12.26	11.25	11.1	11.65	11.68	11.76	12.21	12.17	12.13	12.19	11.87	11.91	11.55	11.78	12.17	12.04	12.23

Table 1. Continued.

Sample	North of Niksar										Ayvaz									
	Alkaline										Alkaline									
	95-39	95-40	95-41	95-42	95-43	0-39	95-29	95-30	95-31	95-32	95-33	95-34	95-35	95-36	95-37	95-38				
SiO <sub>2</sub> wt%	53.23	53.63	53.11	53.01	56.23	54.66	56.51	52.93	54.36	54.56	53.47	53.67	54.55	55.21	53.49	56.27				
TiO <sub>2</sub>	0.96	0.96	0.96	1	0.83	0.95	0.8	0.97	0.95	0.94	0.98	0.99	0.92	0.95	0.95	0.83				
Al <sub>2</sub> O <sub>3</sub>	17.46	17.4	17.3	17.3	17.61	17.25	17.2	17.19	17.41	17.47	17.93	17.92	17.07	17.29	17.43	17.79				
Fe <sub>2</sub> O <sub>3</sub> <sup>s</sup>	7.16	7.06	7.07	7.14	6.5	6.9	6.34	7.17	6.76	6.84	7.24	7.27	6.76	6.85	7	6.46				
MnO	0.13	0.13	0.13	0.13	0.11	0.13	0.12	0.13	0.12	0.12	0.13	0.13	0.12	0.13	0.13	0.11				
MgO	3.8	3.74	3.78	3.84	3.12	3.18	3.26	3.84	3.69	3.68	3.77	3.69	3.09	3.17	3.72	3.34				
CaO	8.46	7.93	8.25	8.51	7.25	7.23	7.26	8.42	7.93	8.14	7.8	7.9	7.28	7.28	8.29	7.3				
Na <sub>2</sub> O	5.02	5.09	5.29	5.32	4.94	5.4	4.89	5.26	5.06	4.96	4.91	4.9	5.32	5.32	4.99	4.97				
K <sub>2</sub> O	2.48	2.44	2.47	2.54	2.39	2.86	2.98	2.53	2.37	2.33	2.47	2.54	2.75	2.73	2.39	2.4				
P <sub>2</sub> O <sub>5</sub>	1.02	0.98	1	1	0.78	1.06	0.75	0.99	0.87	0.86	0.98	0.98	1.03	1.01	0.93	0.78				
LOI	0.31	0.14	0.07	0.09	-0.01	0.62	-0.06	0.01	-0.04	-0.04	0.72	0.54	1	0.5	0.11	-0.05				
Total	100.02	99.52	99.41	99.84	99.74	100.24	99.95	99.44	99.48	99.86	100.4	100.53	99.9	100.45	99.44	100.2				
Rb ppm	46	53	54	54	52	51	48	53	54	52	48	52	53	52	51	50				
Sr	1372	1319	1347	1361	1006	1341	992	1348	1183	1186	1164	1181	1301	1288	1234	1012				
Ba	718	685	688	702	658	786	636	703	659	642	719	712	803	807	696	643				
Nb	56	52	54	52	45	44	42	55	50	49	53	53	44	46	51	43				
Th	10	11	8	11	9	3	8	11	11	11	12	12	8	8	12	9				
Y	24	24	23	25	23	24	22	24	22	22	25	24	24	24	24	23				
Ni	26	26	25	24	22	22	20	23	23	24	29	28	23	23	25	20				
Cr	22	23	22	22	17	8	22	21	25	27	17	20	19	19	18	24				
Pb	21	21	18	19	32	9	21	21	20	18	21	22	18	18	20	20				
V	65	86	100	92	76	46	77	89	86	98	43	82	48	51	92	83				
Zn	87	87	82	79	82	79	80	79	76	77	92	89	79	79	84	74				
Zr	240	231	236	231	233	235	226	238	229	227	240	241	244	246	226	227				
La	71	57	57	61	61	58	57	64	61	57	64	67	64	61	71	57				
Ce	103	110	109	111	22	130	96	111	92	100	124	118	111	107	113	100				
Nd	29	44	44	42	34	53	40	35	32	38	50	42	39	40	50	53				
Zr/Nb	4.29	4.44	4.37	4.44	5.18	5.34	5.98	4.33	4.58	4.63	4.53	4.55	5.55	5.35	4.43	5.28				
Y/Nb	0.43	0.46	0.43	0.48	0.51	0.55	0.52	0.44	0.44	0.45	0.47	0.45	0.55	0.52	0.47	0.53				
Ba/La	10.1	12	12.1	11.5	10.8	13.6	11.2	11	10.8	11.3	11.2	10.6	12.5	13.2	9.8	11.3				
Th/Nb	0.2	0.2	0.1	0.2	0.2	0.1	0.2	0.2	0.2	0.2	0.2	0.2	0.2	0.2	0.2	0.2				
La/Nb	1.3	1.1	1.1	1.2	1.4	1.3	1.4	1.2	1.2	1.2	1.2	1.3	1.5	1.3	1.4	1.3				
Al <sub>2</sub> O <sub>3</sub> /TiO <sub>2</sub>	18.2	18.1	18	17.3	21.2	18.2	21.5	17.7	18.3	18.6	18.3	18.1	18.6	18.2	18.3	21.4				
Na <sub>2</sub> O/K <sub>2</sub> O	2	2.1	2.1	2.1	2.1	1.9	2.1	2.1	2.1	2.1	2	1.9	1.9	1.9	2.1	2.1				
CaO/Al <sub>2</sub> O <sub>3</sub>	0.48	0.46	0.48	0.49	0.41	0.42	0.42	0.49	0.46	0.47	0.44	0.44	0.43	0.42	0.48	0.41				
CaO/TiO <sub>2</sub>	8.81	8.26	8.59	8.51	8.73	7.61	9.08	8.68	8.35	8.66	7.96	7.98	7.91	7.66	8.73	8.8				

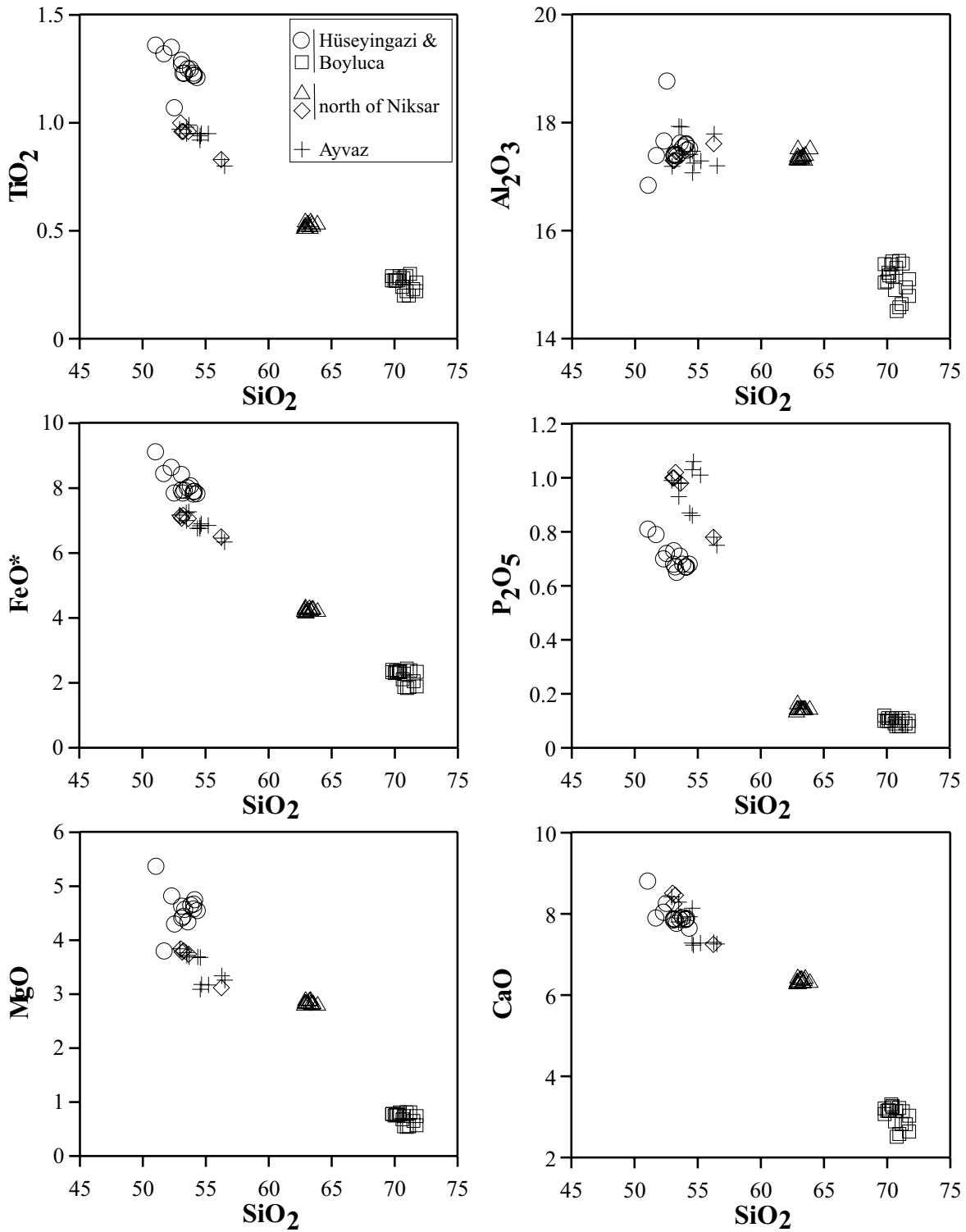


Figure 5. Major oxide vs SiO<sub>2</sub> variation diagrams of the alkaline and sub-alkaline rocks of Niksar Basin.

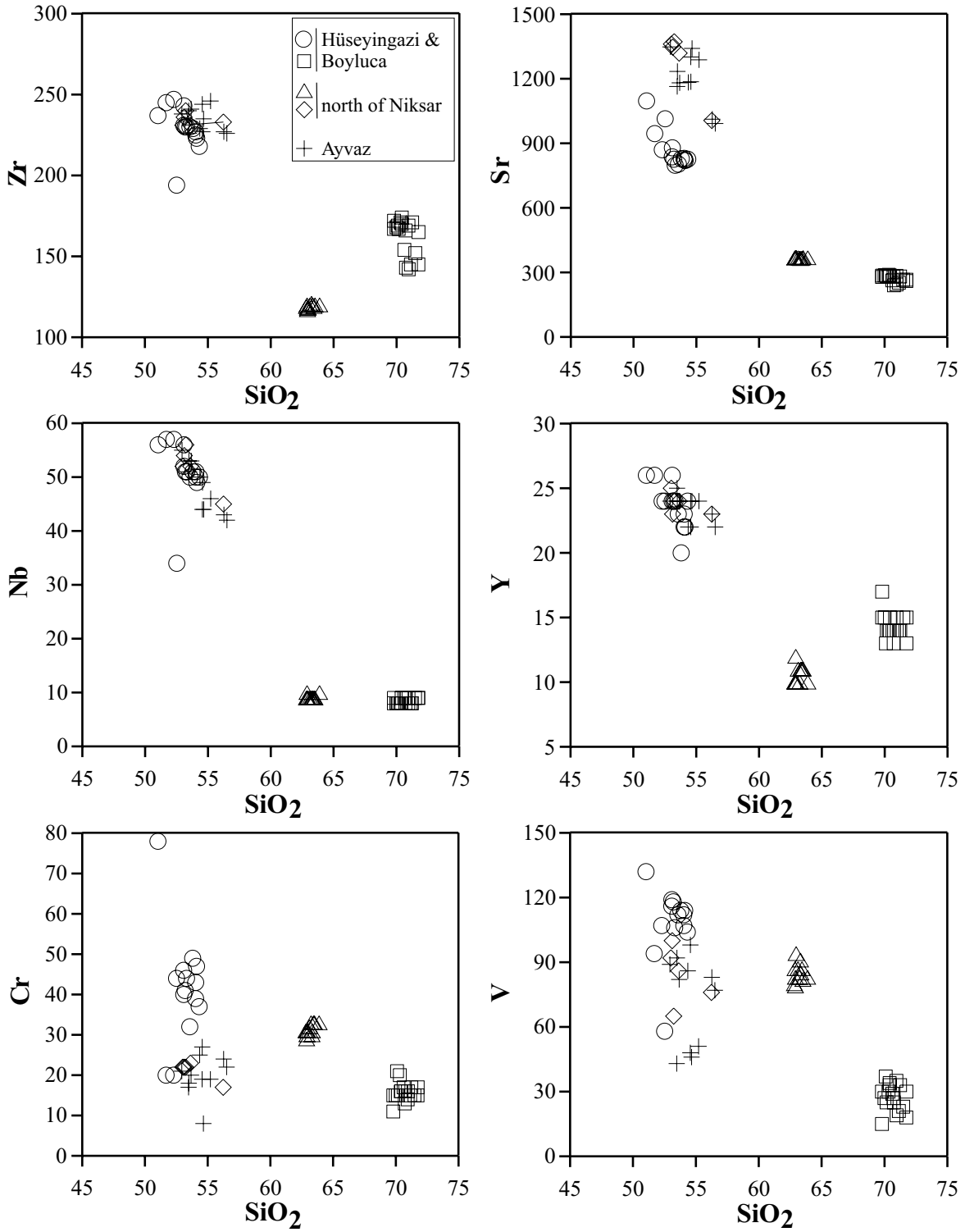


Figure 6. Variation in Zr, Nb, Rb, Sr, Y, Ni, Cr and V with  $\text{SiO}_2$  for the Niksar pull-apart basin alkaline and sub-alkaline volcanic rocks.

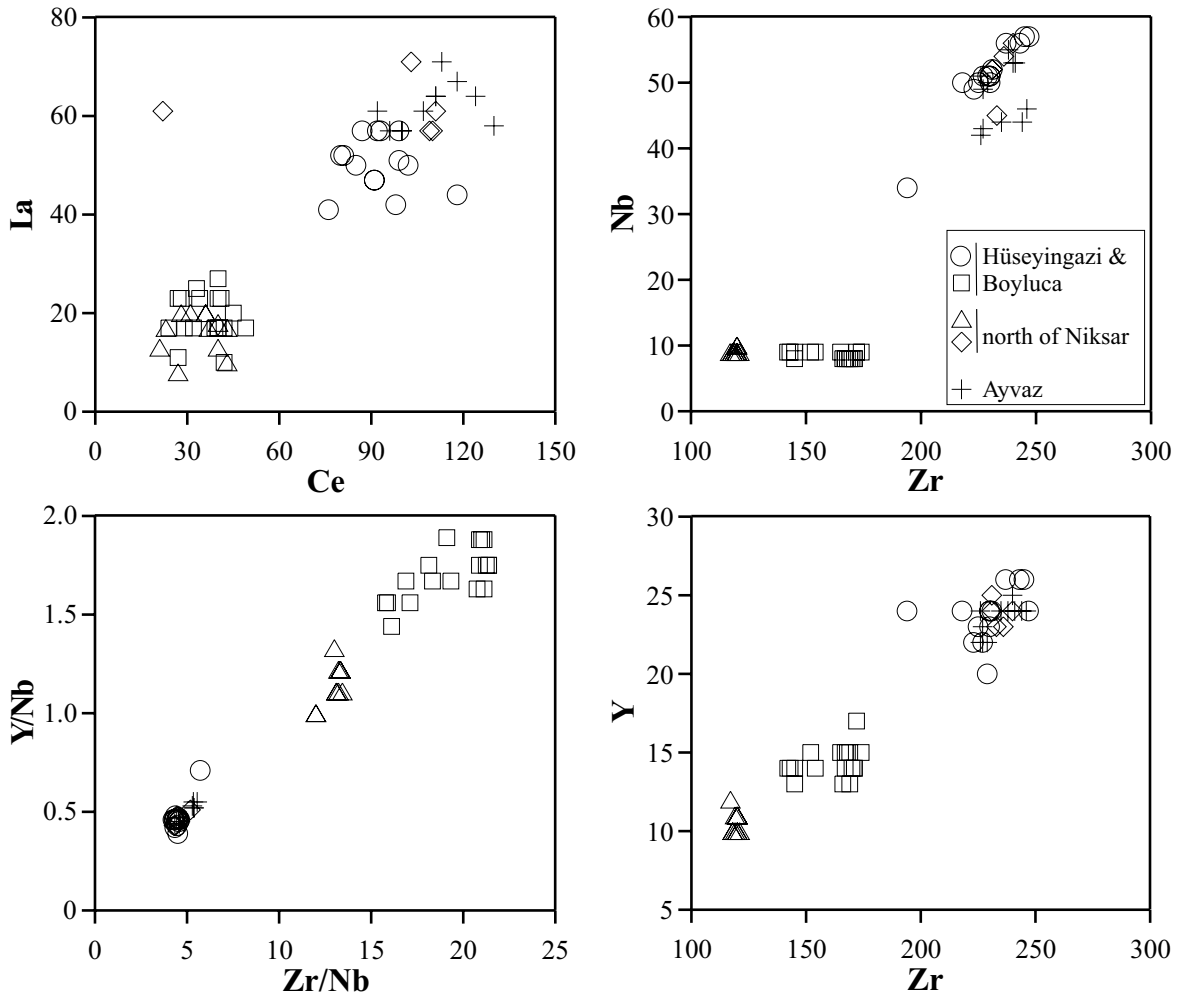


Figure 7. Interelemental variation diagrams of the Niksar Basin volcanic rocks.

localities in Anatolia (Pearce *et al.* 1990; Seyitoğlu *et al.* 1997; Wilson *et al.* 1997; Deniel *et al.* 1998; Aldanmaz *et al.* 2000; Adıyaman *et al.* 2001). The high-silica sub-alkaline group shows LIL enrichment (e.g., higher Th). This may suggest derivation from a subduction-modified source.

The chondrite normalized rare earth element (REE) patterns for the representative samples from each location in the Niksar pull-apart basin are shown in Figure 9. They are all light rare earth element (LREE) enriched typically showing progressive enrichment from Lu to La. Mugearites and benmoreites of Ayvaz and Hüseyingazi-Boyluca lavas display a greater overall REE enrichment than the Niksar andesitic lavas.

Primitive mantle normalized (Sun & McDonough 1989) incompatible trace element concentrations of Niksar pull-apart basin lavas are shown in Figure 10. For comparison typical OIB and MORB trace element patterns are also shown. These patterns are all characterized by significant enrichments in all the large ion lithophile elements (LILE), Rb, Ba, K, Th and the light REE relative to the high field strength elements (HFSE), Nb, Ti, Zr, Y and particularly alkaline basalts of each location show distribution patterns which are typical of ocean island basalt (OIB) lavas with HIMU-like characteristics such as positive Nb anomaly (e.g., St Helena, Bouvet, Ascension; Weaver 1991). However, a positive Ba anomaly is not usually observed in HIMU patterns but is typical of some

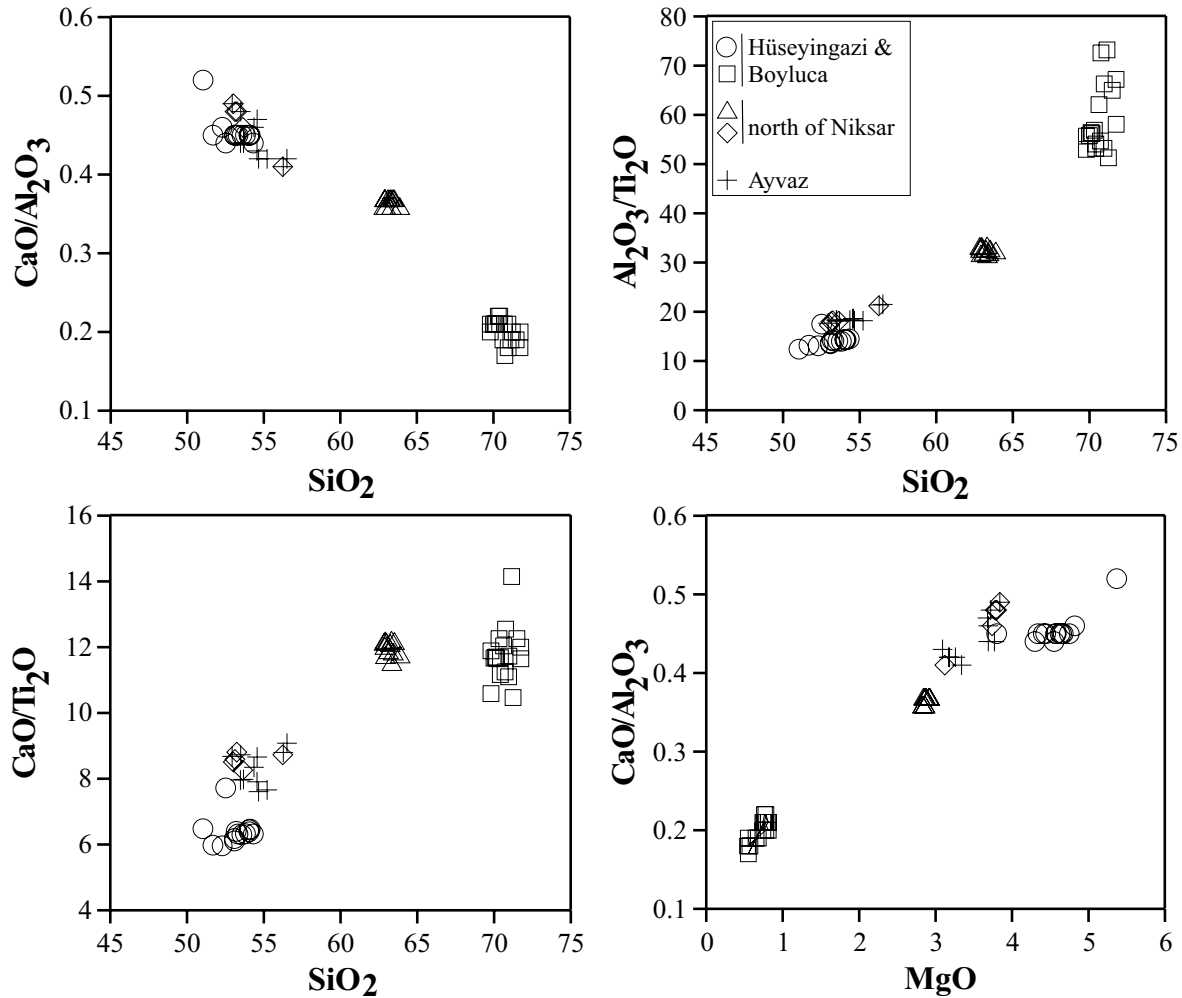


Figure 8.  $\text{CaO}/\text{Al}_2\text{O}_3$ ,  $\text{Al}_2\text{O}_3/\text{TiO}_2$ ,  $\text{CaO}/\text{TiO}_2$  ratios vs  $\text{SiO}_2$  and  $\text{CaO}/\text{Al}_2\text{O}_3$  vs  $\text{MgO}$  diagrams of the Niksar Basin volcanic rocks.

EM1 (Enriched Mantle) lavas (e.g., Weaver 1991). There are some variations in sub-alkaline members of the each series with dacites and rhyolites showing slight negative anomalies in Nb, P, Zr and Ti on their primitive mantle normalized diagrams suggesting crustal contamination during their genesis. These negative Nb anomalies are similar to those from subduction-related (active) continental margins characterised by the involvement of a mantle source metasomatised by fluids enriched in Sr, K, Rb, Ba and Th in their petrogenesis (Pearce 1983). However, the tectonic evolution of the area indicates that Quaternary volcanism in this area has been related to the development of the NAFZ which was initiated sometime

between the Late Miocene and Early Pliocene (e.g., Seymen 1975; Barka & Gülen 1988, Tatar 1993; Barka *et al.* 2000; Bozkurt 2001; Westaway 2003; Şengör *et al.* 2005; Kaymakçı *et al.* 2006; Aksoy *et al.* 2007; Bektaş *et al.* 2007) after the collision between Afro-Arabian and Eurasian plates had begun by the Middle Miocene in eastern Turkey (Barka & Gülen 1988; Barka 1992). The suggested explanations of the LILE and LREE enrichments for collision-related sub-alkaline and alkaline magmas relative to Nb could be either a subduction component inherited from earlier subduction events (Pearce 1983) or crustal contamination through assimilation and fractional crystallization (De Paolo

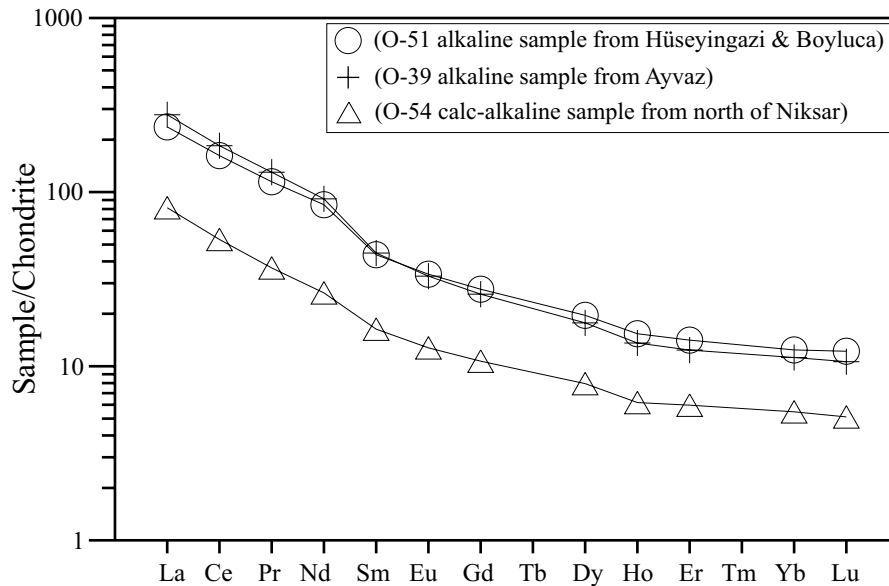


Figure 9. Chondrite normalized REE diagram of alkaline mugearite, benmoreite and sub-alkaline dacite (normalization values from Nakamura 1974).

1981). The high concentrations of Nb relative to Zr and of Zr relative to Y indicate a contribution from upper mantle enriched in incompatible element as is observed in within plate basalts (Pearce 1983).

### Petrogenesis

The close spatial relationship and the contemporaneous extrusion of the different lavas of the Niksar pull-apart basin suggest that these lavas are genetically related. Also the relatively well-established chemical transition between the magma types in Niksar Basin supports the notion that they are products of similar, or possibly even the same, magmatic processes.

### Fractional Crystallization

The relatively well-defined and regular major and trace element variations in the Niksar pull-apart basin lavas with a progressive enrichment of REE from Lu to La from least to the most evolved rocks is a correlation observed only for the alkaline lavas (Figure 7). Their observations are consistent with fractional crystallization and are considered to indicate their co-magmatic origin despite a large gap between basaltic and felsic lavas (cf. Kamber & Collerson 1999). Their MgO contents decreases with increasing SiO<sub>2</sub>. Al<sub>2</sub>O<sub>3</sub> contents increase with increasing

SiO<sub>2</sub> in the undersaturated series and decrease in the saturated series. Furthermore CaO/Al<sub>2</sub>O<sub>3</sub> ratios decrease with increasing SiO<sub>2</sub> whilst Al<sub>2</sub>O<sub>3</sub>/TiO<sub>2</sub> and CaO/TiO<sub>2</sub> ratios increase with increasing SiO<sub>2</sub> (Figure 6). Again there is a very good positive correlation in CaO/Al<sub>2</sub>O<sub>3</sub> vs MgO diagram indicating augite fractionation (Figure 8). Incompatible trace element contents increase whereas Cr and Ni contents decrease with increasing SiO<sub>2</sub>. These features show that the genesis of the Niksar pull-apart basin volcanic rocks is influenced by the crystal fractionation process and the felsic lavas appears to be the result of fractional crystallization processes involving clinopyroxene and plagioclase. The very low abundances (<5 ppm) of transition elements in rhyolites and rhyodacites indicate that clinopyroxene and oxide fractionations completely depleted the basaltic magmas in these elements. The absence of a negative Eu anomaly indicates that low-pressure plagioclase fractionation has not taken place. However, the progressive depletion of Sr and Ba from mugearites through benmoreites and the most evolved rocks indicates plagioclase and alkali feldspar fractionation. Low P and Ti contents as shown by significant negative correlation on binary diagrams and slight negative anomalies on normalized diagrams for andesites through to rhyolites indicates fractionation of apatite (P) and ilmenite (Ti).

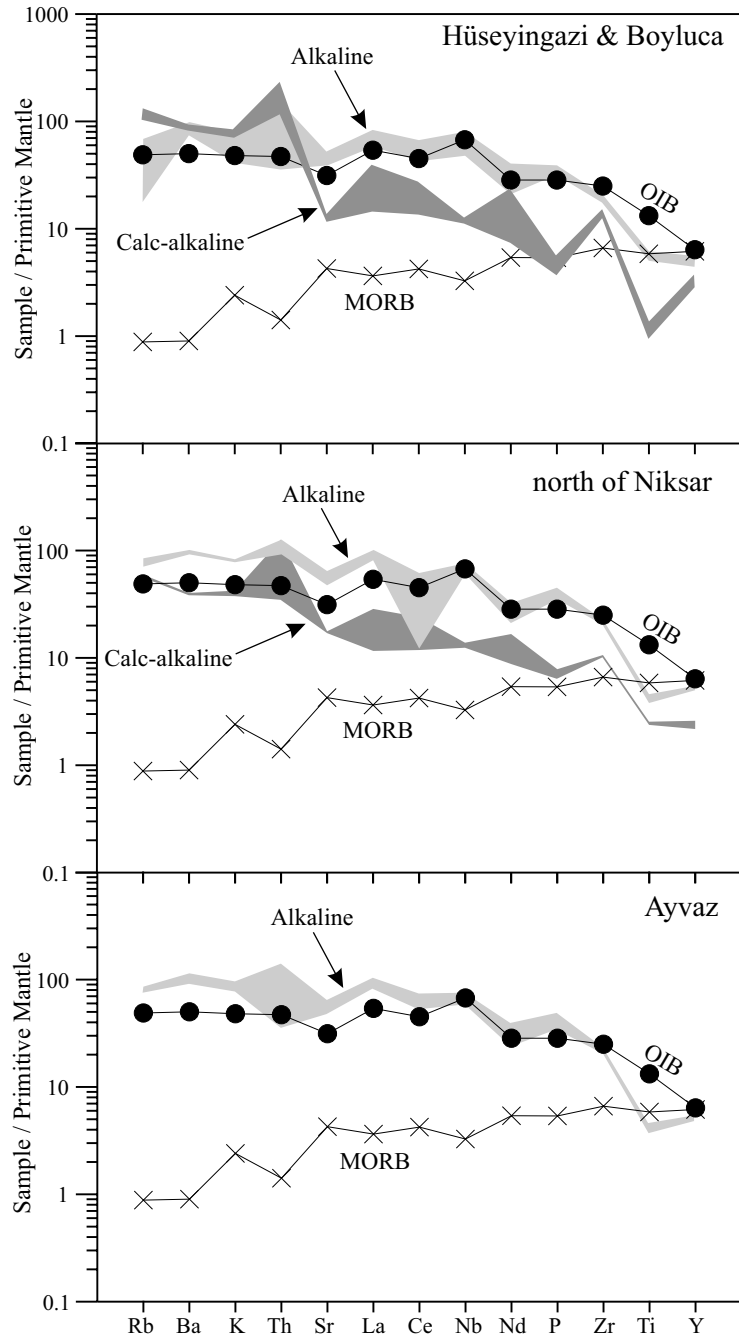


Figure 10. Primitive mantle normalized incompatible trace element patterns of mugearites, benmoreites, dacites, rhyodacites and rhyolites.  $\Delta$ –Hüseyingazi-Boyluca samples;  $\diamond$ – North of Niksar samples; + – Ayvaz location samples. Normalization values from Sun & McDonough (1989).

### Partial Melting

During the generation of basaltic magmas from a peridotite source the  $\text{SiO}_2$  content of the melts is pressure

dependent and increases with decreasing pressure. During decompression the degree of melting will also increase (Jaques & Green 1980). Some major element

ratios (e.g., the  $\text{CaO}/\text{Al}_2\text{O}_3$ ) are strongly affected by the melting conditions. High pressure melting experiments have shown that deep melting expands the stability field of garnet at the expense of olivine, clinopyroxene and this causes a pronounced increase in  $\text{CaO}/\text{Al}_2\text{O}_3$  ratios for liquids that are saturated in clinopyroxene and garnet (Herzberg 1992). Therefore, in agreement with the results of these experimental investigations the decrease of the  $\text{CaO}/\text{Al}_2\text{O}_3$  ratio and the increase of the  $\text{Al}_2\text{O}_3/\text{TiO}_2$  and  $\text{CaO}/\text{TiO}_2$  ratios with increase in  $\text{SiO}_2$  (Figure 8) corresponds to an increase in the degree of partial melting in the Niksar pull-apart volcanic rocks.

The concentration of highly incompatible elements can also be used to identify the partial melting processes in primitive magmas. Trace element ratios with similar degrees of compatibility like  $\text{La}/\text{Nb}$  and  $\text{Zr}/\text{Nb}$  exhibit a regular decrease from basic to acid lavas. Fractionation of alkali feldspar, augite, titanomagnetite assemblage may barely change the  $\text{Zr}/\text{Nb}$  ratio (Baker & McBirney 1985). However, the positive correlations between incompatible element contents and the simultaneous decrease in transition element contents from mugearites-benmoreites to rhyolites and the enrichment of LREE over HREE are in favour of a co-magmatic origin for basaltic and felsic lavas. Therefore, we interpret this variability as not only the fractional crystallization but also as a result of a combination of effects of different degrees of partial melting with different degrees of crustal contamination. We regard low  $\text{Zr}/\text{Nb}$  (~5) and high Sr (~1350) as diagnostic of low-degree partial melting whilst high  $\text{Zr}/\text{Nb}$  may represent higher degree partial melting.

### *Crustal Contamination*

Continental alkaline basalts are often enriched in trace element contents relative to their oceanic counterparts and it is essential to evaluate the possible effects of crustal contamination.  $\text{La}/\text{Nb}$ ,  $\text{Th}/\text{La}$  and  $\text{Ba}/\text{La}$  ratios are thought to be important for identifying crustal contamination of magmas (Thompson *et al.* 1984; Sun & McDonough 1989). The  $\text{La}/\text{Nb}$  ratio of the continental alkali basalts in OIB settings is <1, but in continental basalt provinces the  $\text{La}/\text{Nb}$  ratio ranges between 0.5 and 7 (Thompson *et al.* 1984). The continental crust has  $\text{La}/\text{Nb}>1$  (Taylor & McLennan 1985). The Niksar pull-apart basin volcanic rocks has overall  $\text{La}/\text{Nb}$  ratio ranging

between 0.7 and 3.4 indicating variable degrees of crustal contamination. This ratio is between 1.1 and 3.4 in felsic lavas and between 0.7 and 2.2 in basic lavas. The  $\text{Ba}/\text{La}$  ratio of the primitive mantle is 9.6. In the Niksar pull-apart basin the  $\text{Ba}/\text{La}$  ratio of the basic lavas lies between 9.5 and 15.4 and between 22.5 and 65.1 in felsic lavas indicating significant crustal contamination. High  $\text{Zr}/\text{Nb}$  ratios of felsic lavas (15.78–21.38) compared to the basic lavas (4.23–5.71) are also consistent with crustal contamination.

### *Mantle Source Characteristics*

The depth and nature of the mantle source (either asthenosphere or subcontinental ancient lithosphere) are dominant factors that control the overall characteristics of mantle derived melts. Diagnostic trace element patterns for the mugearites and benmoreites are closely similar to those of ocean island basalts (OIB) with overall high trace element abundances and a peak at Ba and Nb. The spidergrams of the most evolved rhyodacites and rhyolites also show some similarities to OIB fractionated lavas with some relative depletion of Ba, Sr and Ti in the patterns suggesting fractional crystallization of alkali feldspar, plagioclase and Fe-Ti oxides.

Thompson (1986) suggested that all continental alkali basalts with distinct mantle normalized Nb peaks. The asthenospheric mantle component is regarded as a mixture of depleted mantle (DM: depleted MORB-type mantle mixed with plume material) and shows affinities to that of St. Helena OIB source (HIMU). EM is the lithospheric mantle component and has enriched mantle characteristics similar to the source of a Gough-type OIB source (Weaver 1991). Apart from this, a number of recent studies on the origin of OIB-type lavas have been suggested. Aldanmaz *et al.* (2006) stated that alkaline lavas are generated by variable degrees of partial melting of an isotopically homogeneous, single mantle domain enriched in incompatible elements relative to hypothetical Depleted Morb Mantle (DMM) and Primitive Mantle (PM). Pilet *et al.* (2004) suggested that basalts characterized by OIB chemical compositions could be generated by partial melting of metasomatic veins plus enclosing lithospheric mantle. Such a heterogeneous source may form within either the continental or oceanic lithosphere. Lustrino (2005) proposed that delamination and detachment of lower continental crust may be able to bring crustal

lithologies down to mantle depths. The interaction of partial melts derived from these lithologies with ambient mantle can explain some geochemical features of ocean island basalt (OIB) and continental flood basalt (CFB). Anderson (2005) stated that an eclogitic reservoir in the mantle may be a source for the OIB and CFB.

It is usually assumed that incompatible trace element ratios are not strongly fractionated from each other either during partial melting or fractional crystallization. It is shown in Figure 11 that the Ba/Nb and Zr/Nb ratios are not affected for the alkaline basic rocks of mugearites and benmoreites as shown by their decreasing Nb concentrations. Benmoreites show slightly higher Zr/Nb ratios than mugearites. This might be due to the

enrichment of Zr relative to Nb or may be related to fractionation of Zr relative to Nb during partial melting in the presence of garnet (Kamber & Collerson 1999). The Niksar alkaline basic volcanic rocks have Zr/Nb and La/Nb ratios similar to those observed in basalts between HIMU and EM sources (Table 2), suggesting that their sources have a similar geochemical signature (Wilson 1993). An asthenospheric mantle source has also been suggested for the Pliocene–Pleistocene basalts of the Central Anatolian Fault Zone (Parlak *et al.* 2001) and other strike-slip fault related volcanism in southern Turkey (Polat *et al.* 1997; Yurtmen *et al.* 2000).

Taking the available evidence into account we consider that the compositional variations of our samples result

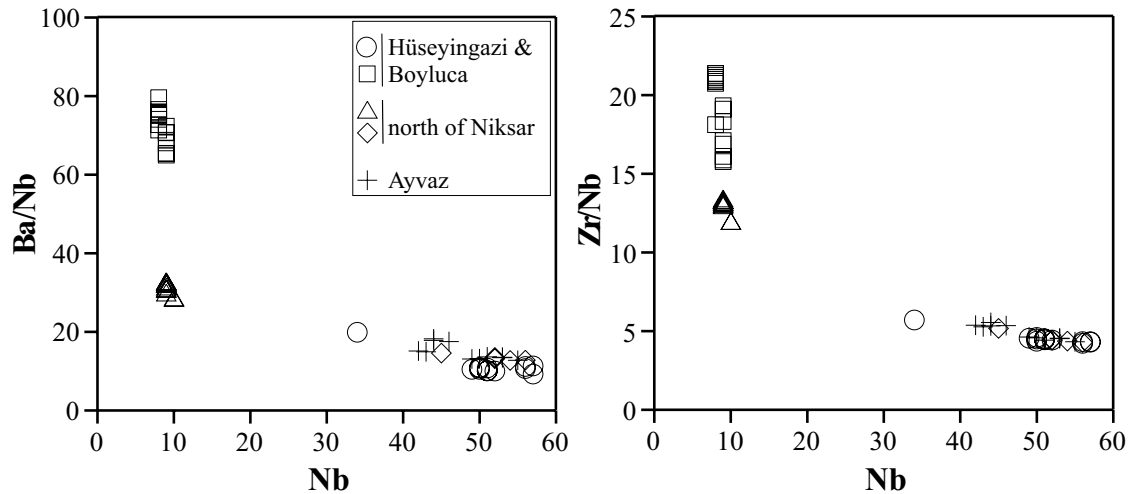


Figure 11. Ba/Nb and Zr/Nb vs Nb diagrams of the Niksar pull-apart basin volcanic rocks.

Table 2. Comparison of trace element composition of the volcanic rocks of the Niksar Basin with ocean island basalts, continental crust and characteristic trace element composition of primordial mantle.

	N-MORB			OIB			NIK SAR BASIN	
	Primordial Mantle	DM Depleted Mantle	Continental crust	HIMU	EM1	EM2	Alkaline	Sub-alkaline
Zr/Nb	14.8	30	16.2	2.7 – 5.5	3.5 – 13.1	4.4 – 7.8	4.2 – 5.7	12 – 21.4
La/Nb	0.94	1.07	2.2	0.64 – 0.82	0.78 – 1.32	0.79 – 1.19	0.7 – 1.5	1.1 – 3.4
Ba/Nb	9	4.03	54	4.7 – 6.9	9.1 – 23.4	6.4 – 13.3	9.3 – 18.3	28.6 – 76.6
Ba/Th	77	60	124	39 – 85	80 – 204	57 – 105	51 – 226	30 – 97
Rb/Nb	0.91	0.36	4.7	0.30 – 0.43	0.69 – 1.23	0.58 – 0.87	0.3 – 1.2	3.7 – 10.5
Th/Nb	0.117	0.07	0.44	0.07 – 0.12	0.09 – 0.13	0.10 – 0.17	0.05 – 0.3	0.3 – 2.2
Th/La	0.125	0.07	0.2	10 – 0.16	0.09 – 0.15	0.11 – 0.18	0.05 – 0.3	0.2 – 1.5
Ba/La	9.6	4	25	6.2 – 9.3	11.3 – 19.1	7.3 – 13.5	9.5 – 15.4	13.5 – 65.1

Data from Wilson (1993)

from a combination of different degrees of partial melting, fractional crystallization and variable degrees of crustal contamination. The magmas that produced the Niksar pull-apart basin volcanic rocks originated from an enriched mantle source similar to the OIB source and were then contaminated by crustal material during the ascent of the magma to produce more evolved felsic counterparts.

### Interpretation of the Tectonic Setting

Cenozoic magmatism in the Pontides was controlled largely by the continental collision between the Pontide and Anatolide plates (Şengör & Kidd 1979; Şengör *et al.* 1980). The age of collision (approximately 10 m.y. ago) and the average convergence rate over this time period (about 4.5 cm/yr; McKenzie 1972) indicate that the slab must long be past the 100–150 km depth where the majority of calc-alkaline and alkaline melts are generated. Pliocene to Recent volcanism is very extensive in the highest part of the east Anatolian convergence plateau and includes both calc-alkaline and alkaline associations, although the former predominate. The calc-alkaline association is represented by andesites, dacites, and rhyolites with some ignimbrites, whereas basalts and very limited phonolites and trachytes represent the alkaline association. Consequently the observations that (i) the Plio–Quaternary volcanic rocks are almost entirely confined to the highest parts of the east Anatolian plateau and that (ii) there is a zone of seismic attenuation beneath the plateau (Toksöz & Bird 1977) support the view that a large portion of the calc-alkaline volcanic rocks might be the product of partial melting of lower levels of the thickened continental crust. In contrast, many recent papers suggest a mantle origin for the East Anatolian volcanism (e.g., Pearce *et al.* 1990; Keskin 2003; Şengör *et al.* 2003).

Aydın *et al.* (1990) point out that magmatic structures such as volcanoes and dykes occur within fault zones at stepovers and are often offset by the faults. Extension perpendicular to the strike-slip faults is evident also by normal faults that are subparallel to the strike-slip faults. They suggested two possible interpretations for this conspicuous relationship; either the strike-slip faults follow weak zones, which in this case are facilitated by the magmatic structures, or magma intrudes into the strike-slip fault zones and the magmatic structures are

deformed and offset as fault displacement continues. The present configuration of the ENE margin of the Niksar Basin is consistent with this idea because the NE–SW extension is almost perpendicular to the NW–SE-trending main strike-slip faults. This extension direction is identified from kinematic analysis of macroscopic–mesoscopic structures and a microcrack study (Tatar 1993). The less abundant alkaline rocks are probably the result of local longitudinal cracking of the crust, under north–south shortening, providing access to the mantle.

Dewey *et al.* (1986) note an interesting contrast between pull-apart basins on the North Anatolian Fault Zone and those on the East Anatolian Fault Zone. From the slip rates of the NAFZ and EAFZ and the lengths of pull-apart basins along them, they propose that strain rate is the reason for this difference; in regions of high extensional strain rate the lithosphere like the NAFZ pull-apart basins may be thinning faster than it thickens by regional shortening and by thermal re-equilibration, thus allowing fertile mantle to rise from depths where partial melting is possible (Figure 8). Alternatively, the dominant calc-alkaline geochemical composition of volcanic rocks near the Niksar pull-apart basin may indicate that the Niksar Basin may be a pull-apart that affects only the elastic lid (Figure 12a).

Adıyaman *et al.* (2001) studied three different regions along the North Anatolian Fault Zone and determined a 900–1000 ka geochronological age for the young volcanic rocks around the Niksar Basin. Isotopic and trace element geochemical data of these volcanic rocks reflect a dominantly lithospheric mantle source, slightly mixed with asthenospheric liquids. Most magmas were fractionated and contaminated by continental crust during their ascent. The authors indicated that the strike-slip movement along the NAFZ began in the Early Pliocene in Niksar and that the NAFZ has served to channel small quantities of asthenospheric melts from the base of the lithosphere.

The geochemical composition of the volcanic rocks in the study area varies from alkaline to calc-alkaline associations with the former predominating over the latter. Harris *et al.* (1986) divided collisional magmatism into four groups as follows: (i) pre-collision calc-alkaline intrusions, (ii) syn-collision peraluminous intrusions, (iii) late or post-collision calc-alkaline intrusions and (iv) post-collision alkaline intrusions. Group (iii), comprising the late or post-collision calc-alkaline intrusions, may be

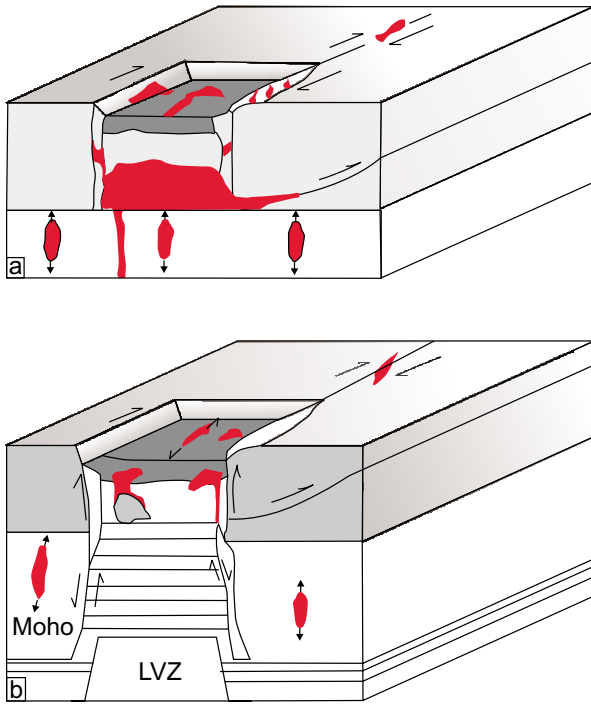


Figure 12. Schematic strike-slip pull-apart basins involving (a) only the elastic lid (basement symbol), and (b) the whole lithosphere (slightly modified from Dewey *et al.* 1986).

derived from a mantle source but undergo extensive crustal contamination. Group (iv), the post-collision alkaline intrusions, may be derived from mantle lithosphere beneath the collision zones and carry high concentrations of both LIL and HFS elements. In this classification, the volcanic rocks in the Niksar area carry dominantly the characteristics of group (iv) and may be group (iii) according to their geochemical composition and tectonic setting (Figure 13).

## Conclusions

The enriched nature of many oceanic and continental intraplate alkaline suites with respect to N-type MORB has been widely attributed to a lower mantle-derived plume component in the source region (Zindler & Hart 1986; Wilson 1993). The Niksar Basin alkaline lavas are geochemically comparable to ocean island basalts. Based on the similar La/Nb and Zr/Nb ratios relative to OIB and trace element enriched characteristics, we suggest that the alkaline members of the Niksar Basin basalts were

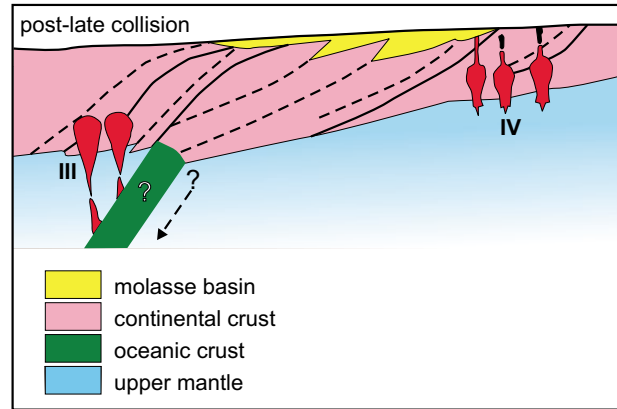


Figure 13. Idealized section of simple post-late collision magmatism in a continent-continent collision. Possible source regions of collision magmatism are indicated for groups III and IV (Harris *et al.* 1986).

derived from a source similar to an asthenospheric HIMU reservoir, together with some interaction with the enriched lithospheric mantle with some crustal contamination. However, the alkaline nature of the volcanism in the the Niksar pull-apart basin is unlikely to be explained by a mantle plume component because, the alkaline volcanic rocks and their evolved counterparts in the area were formed in the localized extensional zones and clearly record strike-slip related transtensional deformation (White & McKenzie 1989) rather than a plume link. They were most likely derived from metasomatized asthenosphere due to decompressional partial melting as a result of fracturing of the continental lithosphere by the North Anatolian strike-slip fault zone (Hawkesworth *et al.* 1990). Alkaline rocks are derived from small degrees of partial melting while the sub-alkaline rocks have been derived from the same or similar mantle sources with greater degrees of partial melting. The mugearites and benmoreites have not been affected greatly by crustal contamination processes but their sub-alkaline differentiates show significant contamination.

Fractional crystallization of the observed phases accounts for the diversity of intermediate and evolved products. Amphibole fractionation in basalts at depth causes the trend towards silica saturation while alkali feldspar fractionation dominates final stages of crystallization. The occurrence of these young volcanic rocks just outside of the basin could be either due to a high rate of sedimentation or the geometry of the basin covering a wider buried region of volcanic rocks.

## Acknowledgment

The authors would like to thank John Winchester and G.T.R. Droop for reviews and suggestions on earlier

version of this manuscript. Osman Parlak is thanked for evaluation of the geochemical data. John Piper edited the English of final text.

## References

- ADİYAMAN, Ö., CHOROWICZ, J., ARNAUD, O.N., GÜNDOĞDU, M.N. & GOURGAUD, A. 2001. Late Cenozoic tectonics and volcanism along the North Anatolian Fault: new structural and geochemical data. *Tectonophysics* **338**, 135–165.
- AKSOY, E., İNCEÖZ, M. & KOÇYİĞİT, A. 2007. Lake Hazar Basin: a negative flower structure on the East Anatolian Fault System (NAFS), SE Türkiye. *Turkish Journal of Earth Sciences* **16**, 323–342.
- ALDANMAZ, E., KÖPRÜBAŞI, N., GÜRER, Ö.F., KAYMAKCI, N. & GOURGAUD, A. 2006. Geochemical constraints on the Cenozoic, OIB-type alkaline volcanic rocks of NW Turkey: Implications for mantle sources and melting processes. *Lithos* **86**, 50–76.
- ANDERSON, D.L. 2005. *The Layered Mantle Revisited: An Eclogite Reservoir*. <http://www.mantleplumes.org/hotslabs.html>.
- ARGER, J., MITCHELL, J. & WESTAWAY, R. 2000. Neogene and Quaternary volcanism of south-eastern Turkey. In: BOZKURT, E., WINCHESTER, J.A. & PIPER, J.D.A. (eds), *Tectonics and Magmatism of Turkey and the Surrounding Area*. Geological Society, London, Special Publications **173**, 459–487.
- AYDIN, A. & NUR, A. 1982. Evolution of pull-apart basins and their scale independence. *Tectonics* **1**, 91–105.
- AYDIN, A., SCHULTZ, R.A. & CAMPAGNA, D. 1990. Fault-normal dilation in pull-apart basins: implications for the relationship between strike-slip faults and volcanic activity. *Annales Tectonicae* **2**, 45–52.
- BAKER, B.H. & MCBIRNEY, A.R. 1985. Liquid fractionation. Part III. Geochemistry of zoned magmas and the compositional effects of liquid fractionation. *Journal of Volcanology and Geothermal Research* **24**, 55–81.
- BARKA, A. 1992. The North Anatolian Fault Zone. *Annales Tectonicae* **6**, 164–195.
- BARKA, A., AKYÜZ, H.S., COHEN, H.A. & WATCHORN, F. 2000. Tectonic evolution of the Nıksar and Taşova-Erbaa pull-apart basins, North Anatolian Fault Zone: their significance for the motion of the Anatolian block. *Tectonophysics* **322**, 243–264.
- BARKA, A. & GÜLEN, L. 1988. New constraints on age and total offset of the North Anatolian Fault Zone: Implications for tectonics of the eastern Mediterranean region. *METU Journal of Pure and Applied Sciences* **21**, 39–63.
- BEKTAŞ, O., EYÜBOĞLU, Y. & MADEN, M. 2007. Different Modes of Stress Transfer in a Strike-slip Fault Zone: an Example From the North Anatolian Fault System in Turkey. *Turkish Journal of Earth Sciences* **16**, 1–12.
- BOZKURT, E. 2001. Neotectonics of Turkey: a synthesis. *Geodinamica Acta* **14**, 3–30.
- BOZKURT, E. & KOÇYİĞİT, A. 1996. The Kazova basin: an active negative flower structure on the Almus fault zone, a splay fault system of the North Anatolian fault zone, Turkey. *Tectonophysics* **265**, 239–254.
- CAS, R.A.F. & WRIGHT, J.V. 1987. *Volcanic Successions, Modern and Ancient*. Allen & Unwin Publications.
- CROWELL, J.C. 1974. Origin of late Cenozoic basins in southern California. In: DICKINSON, W.R. (ed), *Tectonics and Sedimentation*. Society of Economic Paleontologists and Mineralogists, Tulsa, Special Publications **22**, 190–204.
- DE PAOLO, D.J. 1981. Trace element and isotopic effects of combined wall-rock assimilation and fractional crystallization. *Earth and Planetary Science Letters* **53**, 189–202.
- DENIEL, C., AYDAR, E. & GOURGAUD, A. 1998. The Hasan Dağı stratovolcano (Central Anatolia, Turkey): evolution from calc-alkaline to alkaline magmatism in a collision zone. *Journal of Volcanology and Geothermal Research* **87**, 275–302.
- DEWEY, J.F., HEMPTON, M.R., KIDD, W.S.F., ŞAROĞLU, F. & ŞENGÖR, A.M.C. 1986. Shortening of continental lithosphere: the neotectonics of Eastern Anatolia – a young collision zone. In: COWARD, M.P. & RIES, A.C. (eds), *Collision Tectonics*. Geological Society, London, Special Publications **19**, 3–36.
- FITTON, J.G. 1987. The Cameroon line, West Africa: a comparison between oceanic and continental alkaline volcanism. In: FITTON, J.G. & UPTON, B.G.J. (eds), *Alkaline Igneous Rocks*. Geological Society, London Special Publications **30**, 273–291.
- FLOYD, P.A. & CASTILLO, P.R. 1992. Geochemistry and petrogenesis of Jurassic ocean crust basalts, ODP Leg 129, Site 801. In: LARSON, R. & LANCELOT, Y. (eds), *Proceedings of Ocean Drilling Program, Scientific Research* **129**, 361–388.
- HARRIS, N.B.W., PEARCE, J.A. & TINDLE, A.G. 1986. Geochemical characteristics of collision zone magmatism. In: COWARD, M.P. & RIES, A.C. (eds), *Collision Tectonics*. Geological Society, London, Special Publications **19**, 67–81.
- HAWKESWORTH, C.J., KEMPTON, P.D., ROGERS, N.W., ELLAM, R.M. & VAN CALSTEREN, P.W. 1990. Continental mantle lithosphere and shallow level enrichment processes in the Earth's mantle. *Earth and Planetary Science Letters* **96**, 256–268.
- HERZBERG, C. 1992. Depth and degree of melting of komatiites. *Journal of Geophysical Research* **97**, 4521–4540.
- IRVINE, T.N. & BARAGAR, W.R.A. 1971. A guide to the chemical classification of the common volcanic rocks. *Canadian Journal of Earth Sciences* **8**, 523–548.

- JAQUES, A.L. & GREEN, D.H. 1980. Anhydrous melting of peridotite at 0–15 Kb pressure and the genesis of tholeiitic basalts. *Contributions to Mineralogy and Petrology* **73**, 287–310.
- KAMBER, B.S. & COLLERSON, K.D. 1999. Zr/Nb Systematics of ocean island basalts reassessed – the case for binary mixing. *Journal of Petrology* **11**, 1007–1021.
- KAYMAKCI, N., İNCEÖZ, M. & ERTEPINAR, P. 2006. 3D-architecture and Neogene evolution of the Malatya basin: inferences for the kinematics of the Malatya and Ovacik fault zones. *Turkish Journal of Earth Sciences* **15**, 123–154.
- KESKİN, M. 2003. Magma generation by slab steepening and breakoff beneath a subduction-accretion complex: An alternative model for collision-related volcanism in Eastern Anatolia, Turkey. *Geophysical Research Letters* **30**, doi: 10.1029/2003GL018019.
- KETİN, İ. 1969. Kuzey Anadolu Fayı Hakkında [About North Anatolian Fault]. *Mineral Research and Exploration Institute (MTA) of Turkey Bulletin* **72**, 1–27 [in Turkish with English abstract].
- KOÇYİĞİT, A. 1989. Süşehri basin: an active fault-wedge basin on the North Anatolian Fault Zone, Turkey. *Tectonophysics* **167**, 13–29.
- LE BAS, M.J., LE MAITRE, R.W., STRECKEISEN, A. & ZANETTIN, B. 1986. A chemical classification of volcanic rocks based on the total alkali – silica diagram. *Journal of Petrology* **27**, 745–750.
- LUSTRINO, M. 2005. How the delamination and detachment of lower crust can influence basaltic magmatism. *Earth Science Reviews* **72**, 21–38.
- McKENZIE, D. 1972. Active tectonics of the Mediterranean region. *Geophysical Journal of Royal Astronomical Society* **30**, 109–185.
- NAKAMURA, Y. 1974. Determination of REE, Ba, Fe, Mg, Na and K in carbonaceous and ordinary chondrites. *Geochimica Cosmochimica Acta* **38**, 757–773.
- PARLAK, O., DELALOYE, M., DEMİRKOL, C. & ÜNLÜGENCE, U.C. 2001. Geochemistry of Pliocene/Pleistocene basalts along the Central Anatolian fault zone (CAFZ), Turkey. *Geodinamica Acta* **14**, 1–9.
- PARLAK, O., KOP, A., ÜNLÜGENCE, U.C. & DEMİRKOL, C. 1998. Geochronology and geochemistry of basaltic rocks in the Karasu Graben around Kırıkhan (Hatay), S. Turkey. *Turkish Journal of Earth Sciences* **7**, 53–61.
- PARLAK, O., KOZLU, H., DEMİRKOL, C. & DELALOYE, M. 1997. Intracontinental Plio–Quaternary volcanism along the African–Anatolian plate boundary, southern Turkey. *Ofioliti* **22**, 1–117.
- PAVONI, N. 1961. Die Nordanatolische Horizontalverschiebung. *Geologische Rundschau* **52**, 122–139.
- PEARCE, J.A. 1983. The role of the sub-continental lithosphere in magma genesis at active continental margins. In: HAWKESWORTH, C.J. & NORRIS, M.J. (eds), *Continental Basalts and Mantle Xenoliths*, 230–249. Nantwich, Shiva.
- PEARCE, J.A., BENDER, J.F., DE LONG, S.E., KIDD, W.S.F., LOW, P.J., GÜNER, Y., ŞAROĞLU, F., YILMAZ, Y., MOORBATH, S. & MITCHELL, J.G. 1990. Genesis of collision volcanism in Eastern Anatolia, Turkey. *Journal of Volcanology and Geothermal Research* **44**, 189–229.
- PILET, S., HERNANDEZ, J., BUSSY, F. & SYLVESTER, P.J. 2004. Short-term metasomatic control of Nb/Th ratios in the mantle sources of intraplate basalts. *Geology* **32**, 113–116.
- PIPER, J.D.A., MOORE, J., TATAR, O., GÜRSOY, H. & PARK, R.G.P. 1996. Palaeomagnetic study of crustal deformation across an intracontinental transform: the North Anatolian Fault Zone in Northern Turkey. In: MORRIS, A. & TARLING, D.H. (eds), *Palaeomagnetism and Tectonics of the Eastern Mediterranean Region*. Geological Society, London, Special Publications **105**, 299–310.
- POLAT, A., KERRICH, R. & CASEY, J.F. 1997. Geochemistry of Quaternary basalts erupted along the east Anatolian and Dead Sea fault zones of southern Turkey: implications for mantle sources. *Lithos* **40**, 55–68.
- ŞAROĞLU, F. 1985. *Doğu Anadolu'nun Neotektonik Dönemde Jeolojik ve Yapısal Evrimi [Geological and Structural Evolution of Eastern Anatolia During Neotectonic Period]*. PhD Thesis, İstanbul University [in Turkish with English abstract, unpublished].
- ŞENGÖR, A.M.C. & KIDD, W.S.F. 1979. Post-collisional tectonics of the Turkish–Iranian plateau and a comparison with Tibet. *Tectonophysics* **55**, 361–376.
- ŞENGÖR, A.M.C., ÖZEREN, S., GENÇ, T. & ZOR, E. 2003. East Anatolian high plateau as a mantle-supported, north–south shortened domal structure. *Geophysical Research Letters* **30**, doi: 10.1029/2003GL017858.
- ŞENGÖR, A.M.C., TÜYSÜZ, O., İMREN, C., SAKINÇ, M., EYİDOĞAN, H., GÖRÜR, N., LE PICHON, X. & RANGIN, C. 2005. The North Anatolian Fault: A new look. *Annual Review of Earth and Planetary Sciences* **33**, 37–112.
- ŞENGÖR, A.M.C., YILMAZ, Y. & KETİN, İ. 1980. Remnants of a pre-Late Jurassic ocean in northern Turkey: Fragments of Permian–Triassic Paleo-Tethys? *Geological Society of American Bulletin* **91**, 599–609.
- SEYİTOĞLU, G., ANDERSON, D., NOWELL, G. & SCOTT, B. 1997. The evolution from Miocene potassic to Quaternary sodic magmatism in western Turkey: Implications for enrichment processes in the lithospheric mantle. *Journal of Volcanology and Geothermal Research* **76**, 127–147.
- SEYMEN, İ. 1975. *Kelkit Vadisi Kesiminde Kuzey Anadolu Fay Zonu'nun Tektonik Özellikleri [Tectonic Characteristics of the North Anatolian Fault Zone in Kelkit Valley]*. PhD Thesis, İstanbul Technical University Publications [in Turkish with English abstract].
- SUN, S.S. & McDONOUGH, W.F. 1989. Chemical isotopic systematics of oceanic basalts: implications for mantle composition and processes. In: SAUNDERS, A.D. & NORRIS, M.J. (eds), *Magmatism in Ocean Basins*. Geological Society, London, Special Publications **42**, 313–345.
- TATAR, O. 1993. *Neotectonic Structures in the East Central Part of the North Anatolian Fault Zone, Turkey*. PhD Thesis, Keele University [unpublished].

- TATAR, O., PARK, R.G., TEMİZ, H. & TUTKUN, S.Z. 1990. Transtensional and transpressional structures associated with the North Anatolian strike-slip fault zone around the Niksar basin. *Proceedings Book, International Earth Sciences Congress on Aegean Regions II*, 323–333.
- TATAR, O., PIPER, J.D.A., PARK, R.G. & GÜRİSOY, H. 1995. Palaeomagnetic study of block rotations in the Niksar overlap region of the North Anatolian Fault Zone, central Turkey. *Tectonophysics* **244**, 251–266.
- TATAR, O., YURTMEN, S., ROWBOTHAM, G., LEES, G. & TUTKUN, S.Z. 1992. The intracontinental young volcanism related to strike-slip deformation in the Z-shaped pull-apart Niksar basin, Turkey. *Abstracts, 29<sup>th</sup> International Geological Congress, Kyoto, Japan 1*, p. 234.
- TATAR, Y. 1978. Kuzey Anadolu Fay Zonu'nun Erzincan-Refahiye arasındaki bölümü üzerinde tektonik incelemeler [Tectonic investigation of the North Anatolian Fault Zone in the area between Erzincan and Refahiye]. *Yerbilimleri* **4**, 201–236 [in Turkish with English abstract].
- TAYLOR, S.R. & McLENNAN, S.M. 1985. *The Continental Crust: Its Composition and Evolution*. Blackwell, Oxford.
- THOMPSON, R.N. 1986. Sources of basic magmas. *Nature* **319**, 448–449.
- THOMPSON, R.N., MORRISON, M.A., HENDRY, G.L. & PARRY, S.J. 1984. An assessment of the relative roles of a crust and mantle in magma genesis: an elemental approach. *Philosophical Transactions of Royal Society, London, Serie A* **310**, 549–590.
- TOKSÖZ, M.N. & BIRD, 1977. Formation and evolution of marginal basins and continental plateaus. In: TALWANI, M. & PITMAN, W.C. (eds), *Island Arcs, Deep Sea Trenches, and Back-Arc Basins*. AGU Maurice Ewing Serie 1, 379–394.
- WEAVER, B.L. 1991. The origin of ocean island basalt end-member compositions: trace element and isotopic constraints. *Earth and Planetary Science Letters* **104**, 381–397.
- WEAVER, C.S. & HILL, D.P. 1979. Earthquake swarms and local crustal spreading along major strike-slip faults in California. *Pure Applied Geophysics* **117**, 51–64.
- WESTAWAY, R. 2003. Kinematics of the Middle East and Eastern Mediterranean updated. *Turkish Journal of Earth Sciences* **12**, 5–46.
- WHITE, R. & MCKENZIE, D. 1989. Magmatism at rift zones: the generation of volcanic continental margins and flood basalts. *Journal of Geophysical Research* **94**, 7685–7729.
- WILSON, M. 1989. *Igneous Petrogenesis. A Global Tectonic Approach*. Unwin Hyman Ltd., London.
- WILSON, M. 1993. Geochemical signatures of oceanic and continental basalts: a key to mantle dynamics? *Journal of Geological Society, London* **150**, 977–990.
- WILSON, M. & DOWNES, H., 1991. Tertiary–Quaternary extension-related alkaline magmatism in Western and Central Europe. *Journal of Petrology* **32**, 811–849.
- WILSON, M., ROSENBAUM, J.M. & DUNWORTH, E.A. 1995. Melilitites: partial melts of the thermal boundary layer? *Contributions to Mineralogy and Petrology* **119**, 181–196.
- WILSON, M., TANKUT, A. & GÜLEÇ, N. 1997. Tertiary volcanism of the Galatia province, north-west central Anatolia, Turkey. *Lithos* **42**, 105–121.
- YURTMEN, S., ROWBOTHAM, G., İŞLER, F. & FLOYD, P. 2000. Petrogenesis of Quaternary alkali volcanics, Ceyhan - Turkey. In: BOZKURT, E., WINCHESTER, J.A. & PIPER, J.D.A. (eds), *Tectonics and Magmatism of Turkey and the Surrounding Area*. Geological Society, London, Special Publications **173**, 489–512.
- ZINDLER, A. & HART, S. 1986. Chemical geodynamics. *Annual Review of Earth and Planetary Sciences* **14**, 493–570.

*Received 02 July 2006; revised typescript received 06 April 2007; accepted 25 April 2007*